ABSTRACT

PEAK TO AVERAGE POWER RATIO REDUCTION IN STBC MIMO-OFDM

Kishor Gannamaneni, M.S.
Department of Electrical Engineering
Northern Illinois University, 2014
Dr. Mansour Tahernezhadi, Director

Orthogonal frequency division multiplexing (OFDM) is an advanced 3G/4G scheme which achieves high data rate and combats multipath fading. However, OFDM systems suffer from nonlinear peak to average power ratio (PAPR) and carrier frequency offsets (CFO). These two factors lead to degraded performance and thereby reducing the system efficiency. OFDM with multiple antennas both at transmitter and receiver and space-time block coding is used to increase the channel capacity and receiver diversity. Space-time block coding is used to increase data rate and for reliable communications. With space-time block coding we can take advantage of both space and time. It is also possible to implement spatial multiplexing using space-time block coding. However, MIMO-OFDM also suffers from high PAPR value. Many methods have been proposed to reduce the PAPR problem in OFDM. Distortion techniques, coding techniques and scrambling techniques are some of those methods. These methods can be extended to MIMO-OFDM. Distortion techniques can reduce the PAPR, but in turn it increases bit error rate. Coding techniques have limitations with number of subcarriers. Scrambling techniques can reduce the PAPR effectively. In this paper we used SLM and PTS methods to reduce the PAPR problem in MIMO-OFDM. The bit error rate performance for each method is plotted and compared with each other. BER performance of MIMO is compared with SIMO and MISO.

NORTHERN ILLINOIS UNIVERSITY

DEKALB, ILLINOIS

DECEMBER 2014

PEAK TO AVERAGE POWER RATIO REDUCTION IN STBC MIMO-OFDM

BY

KISHOR GANNAMANENI

A THESIS SUBMITTED TO THE GRADUATE SCHOOL

IN PARTIAL FULFILLMENT OF THE REQUIREMENTS

FOR THE DEGREE

MASTER OF SCIENCE

DEPARTMENT OF ELECTRICAL ENGINEERING

Thesis Director:

Dr. Mansour Tahernezhadi

ACKNOWLEDGEMENTS

I am extremely grateful to my advisor, Dr. Mansour Tahernezhadi, for his consistent guidance, patience, encouragement and valuable advice during my master's program. It has been a great learning and enjoyable experience to be a Master of Science student in the Department of Electrical Engineering at Northern Illinois University, DeKalb, Illinois,

I would like to thank Dr. Abhijit Gupta and Dr. Donald Zinger, my research committee members, for their valuable suggestions and precious time. I also like to thank Dr. Lichuan Liu, my committee member, for her valuable suggestions during my proposal.

I would like to thank Dr. Hamid Bateni for his support during my second semester at NIU. His ideas made me think out of box, leading to my successful completion of my thesis.

I would like to thank my parents for their unconditional love and support. Special thanks to my brother and friends for their constant motivation.

TABLE OF CONTENTS

Page

LIST OF TABLES

Page

LIST OF FIGURES

Page

Page

CHAPTER 1: INTRODUCTION

1.1 Background

Wireless communication has been one of the major areas of focus since the late 20th century. The demand for large bandwidth and high communication speed is growing at a rapid pace. Due to the increased demand in mobile applications, next-generation wireless mobile system is designed in such a way that they not only support voice call but also provide high-performance data applications over radio-wave communication system [1]. In order to satisfy these demands, wireless technologies like GSM, OFDM, UWB, LTE, XLTE and LTE-A came into existence.

3G mobile communication systems were modeled using the code division multiple access (CDMA) scheme. OFDM technology is the basis for 4G wireless communication systems. 4G wireless technologies like LTE, LTE-A and worldwide interoperability for microwave access (Wi-MAX) operate in the 2-4 GHz frequency region and provide data rates of 100-200 Mbps. Communication takes place in two ways: uplink and downlink. Verma and Sharma [2] state that "the uplink represents the transmission from a mobile terminal to base station, and downlink represents the transmission from a base station to mobile terminal" (p. 2207). With a wider transmission bandwidth, the signal bandwidth becomes greater than the coherence bandwidth leading to inter-symbol interference (ISI) caused by frequency selectivity of the wireless channel which becomes more serious in a single-carrier communication system [3]. One way to counter effects of frequency selectivity is to use a multicarrier technique which divides the total channel

bandwidth into smaller bandwidth portions [3]. OFDM satisfies this requirement as it is a multicarrier system. In order to increase the diversity gain and channel capacity, OFDM with multiple antennas and space-time block coding is used. However, OFDM system has its own disadvantages. It suffers from high PAPR and also has very high sensitivity to CFO.

1.2 Problem Statement

OFDM signal is the superposition of all the individual signals placed on each subcarrier. The superposition leads to a high peak value compared to the average signal value. This leads to a high PAPR value. PAPR value increases as the number of subcarriers increases, and it does not depend on the modulation scheme used. Presence of high peak power signals in the transmitter requires high-power semiconductor amplifiers with large operating region. Designing and implementing such power amplifiers is very costly and also leads to performance degradation. Large peak values force the power amplifiers to go into the saturation region where the signal gets clipped. In this region, the orthogonal nature of the subcarriers is lost, which leads to inter-carrier interference (ICI). The situation is even worse when Doppler combined with multipath propagation is present in the system.

OFDM with multiple antennas at both transmitter and receiver are used to increase channel capacity and spatial diversity. However, MIMO also suffers from high PAPR value which causes signal distortion. PAPR reduction methods proposed for OFDM can be extended to space-time block-coded (STBC) MIMO-OFDM. Many methods have been proposed before to reduce the PAPR. Some of them include signal distortion methods like clipping and filtering, tone injection method, coding techniques like linear block codes and signal scrambling

techniques. Signal distortion techniques can reduce PAPR, but it reduces the BER performance. Coding techniques can also be implemented to reduce the PAPR, but they are limited with number of subcarriers. In this thesis we are implementing scrambling techniques to reduce the PAPR, and performance of each method is compared with each other.

1.3 Thesis Structure

This thesis is framed as follows:

- In Chapter 2, multipath propagation and Doppler effect are studied. The wireless channel characteristics are explained in detail and modeled.
- Chapter 3 deals with the advantages of multicarrier over single-carrier modulation techniques. OFDM system is explained in detail, listing the advantages and drawbacks.
- Chapter 4 explains about the space-time block-coded MIMO-OFDM and Alamouti coding techniques.
- Chapter 5 explains about the PAPR problem in OFDM systems and MIMO-OFDM.
- In Chapter 6, the space-time block-coded MIMO-OFDM system is described and the PAPR reduction techniques are discussed.
- Chapter 7 contains the simulation results for the methods mentioned in Chapter 6 and the results are analyzed in this chapter.
- In Chapter 8, the thesis is concluded, and possible future work is suggested.

CHAPTER 2: WIRELESS CHANNEL MODELLING

2.1 Multipath Propagation

The received signal at the antennas is the summation of different copies (of the same signal) at different times due to attenuations in different paths. These copies add up at the receiver either constructively or destructively, which leads to either constructive or destructive interference. Multipath occurs due to reflections from buildings, mountains, water bodies, etc. Air is the medium or channel of propagation in wireless communications. Multipath propagation causes errors and hence it degrades the performance of communication. The transmitted signal is represented as x(t), received signal as y(t) and the channel as h(t). The relation between the three parameters is shown in Figure 2.1.

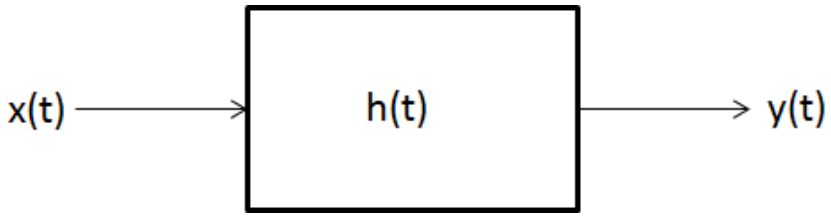

Figure 2.1: Relation between x, h and y.

A circumstance where the signal reaches the receiver through a direct path and L multipath can be observed in Figure 2.2. Direct path is otherwise called line of sight (LOS) and indirect path is named as non-line of sight (NLOS). Equation 2.1 demonstrates the impulse response of the channel.

$$h(t) = a_0\delta(t-\tau_0) + a_1\delta(t-\tau_1) + a_2\delta(t-\tau_2) + \cdots + a_L\delta(t-\tau_L) \quad (2.1)$$

a_L and τ_L are the attenuation and delay associated with L^{th} path [4].

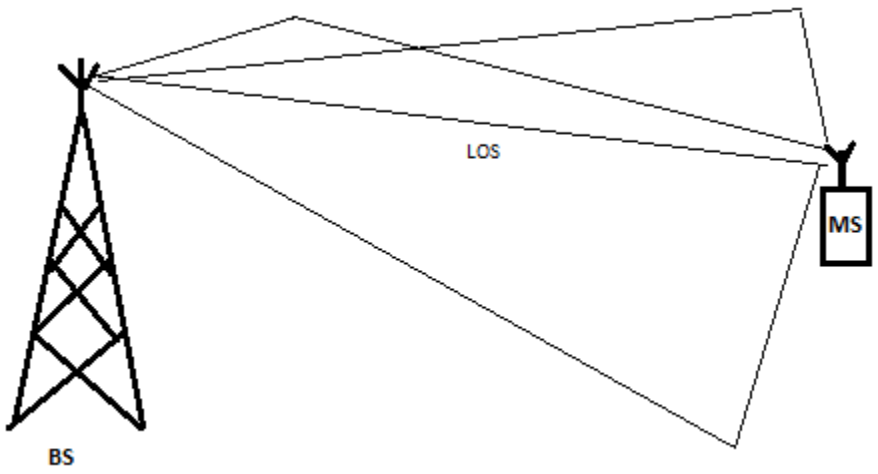

Figure 2.2: Multipath communication.

Equation 2.1 can be further simplified as shown in equation 2.2.

$$h(t) = \sum_{i=0}^{L-1} a_i \delta(t - \tau_i) \tag{2.2}$$

The wireless signal S(t) whose carrier signal is f_c is given by equation 2.3.

$$S(t) = Re\{S_b(t) e^{j2\pi f_c t}\} \tag{2.3}$$

$S_b(t)$ is known as the complex baseband equivalent. The net signal obtained at the receiver combined with the multipath is given by equation 2.4.

$$y(t) = Re\{\sum_{i=0}^{L-1} (a_i S_b(t - \tau_i))$$

$$y_b(t) = \sum_{i=0}^{L-1} a_i S_b(t - \tau_i) \tag{2.4}$$

In practical applications, the value of τ_i is on the order of a few microseconds (~1μs). A signal is said to be a narrow band signal if

$$f_m < \frac{1}{\tau_i} \tag{2.5}$$

For a narrow band signal $S_b(t - \tau_i) = S_b(t)$

$$y_b(t) = S_b(t) \sum_{i=0}^{L-1} a_i e^{-j2\pi f_c \tau_i} \quad (2.6)$$

Equation 2.6 indicates the phenomenon called fading in which we receive a collection of variable power signals at the receiver in feasible applications [4]. 'h' is the fading coefficient and it is determined in equation 2.7 as follows:

$$h = \sum_{i=0}^{L-1} a_i e^{-j2\pi f_c \tau_i} \quad (2.7)$$

2.2 Statistics of Fading Coefficient

The fading coefficient given by equation 2.7 can be split into two random variables. One random variable is real while the other is imaginary. It is shown in equations 2.8 and 2.9.

$$h = \sum_{i=0}^{L-1} a_i e^{-j2\pi f_c \tau_i} = X + jY = ae^{j\varphi} \quad (2.8)$$

$$h = \sum_{i=0}^{L-1} (a_i \cos(2\pi f_c \tau_i) - j a_i \sin(2\pi f_c \tau_i)) \quad (2.9)$$

Upon splitting these terms and assigning them to the two random variables, we get the following results:

$$X = \sum_{i=0}^{L-1} a_i \cos 2\pi f_c \tau_i \text{ and } Y = \sum_{i=0}^{L-1} a_i \sin 2\pi f_c \tau_i$$

The probability density function of the two random variables is given by equation 2.10 [4].

$$f_{A,\varphi} = \frac{1}{\pi} e^{-a^2} \det(J_{XY}) \quad (2.10)$$

J is called as the Jacobian matrix. Let us assume $x = a\cos\varphi; y = a\sin\varphi$:

$$x^2 + y^2 = a^2$$

$$J = \begin{bmatrix} \frac{\partial X}{\partial a} & \frac{\partial Y}{\partial a} \\ \frac{\partial X}{\partial \varphi} & \frac{\partial Y}{\partial \varphi} \end{bmatrix} = \begin{bmatrix} \cos\varphi & \sin\varphi \\ -a\sin\varphi & a\cos\varphi \end{bmatrix}$$

$$\therefore f_{A,\varphi} = \frac{a}{\pi} e^{-a^2} \tag{2.11}$$

The probability distribution function is given by equation 2.12 which is the marginal of the density function with respect to 'a' over a fixed interval.

$$f_A(a) = \int_{-\pi}^{\pi} f_{A,\varphi}(a,\varphi)d\varphi = \int_{-\pi}^{\pi} \frac{a}{\pi} e^{-a^2} d\varphi$$

$$f_A(a) = 2ae^{-a^2} \qquad 0 \le a \le \infty \tag{2.12}$$

The envelope of fading power is demonstrated in equation 2.1 which is broadly known as Rayleigh fading. Rayleigh fading happens because of the multipath propagation in the wireless channel. Fading in the multipath environment is proportional to the Rayleigh distribution. Rayleigh distribution is observed in Figure 2.3.

The probability density of 'a' and φ are given by equations 2.13 and 2.14.

$$2ae^{-a^2} \qquad 0 \le a \le \infty \tag{2.13}$$

$$\frac{1}{2\pi} \qquad -\pi \le \varphi \le \pi \tag{2.14}$$

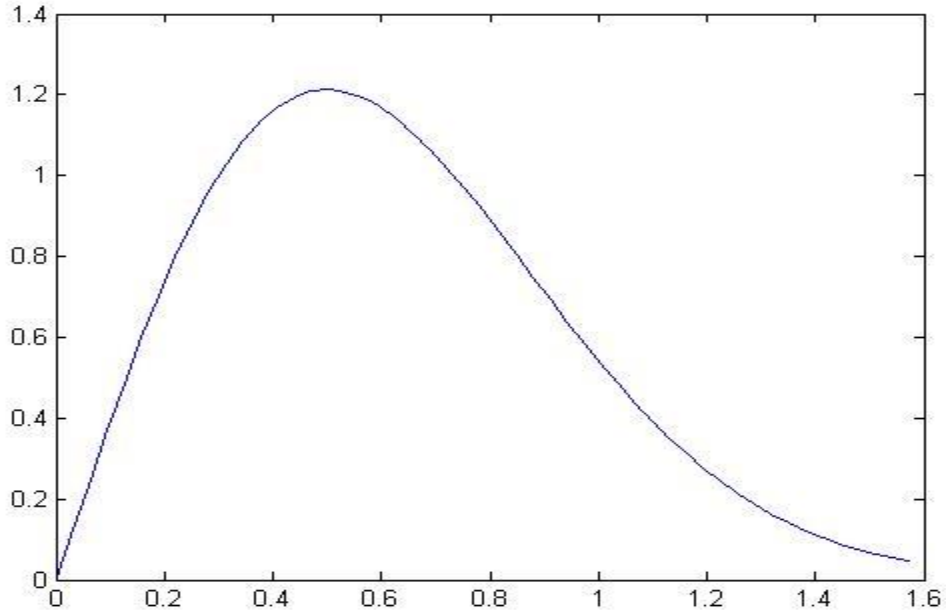

Figure 2.3: Rayleigh distribution.

2.3 Delay Spread

The concept of fading coefficient has been discussed in section 2.2. This section describes the power characteristics and delay spread of the channel. An instance of four multipath channels is considered in which the gain and delay associated with each path are given in Table 2.1. as follows:

Table 2.1: Gain and Delay Values

Gain(g)	Delay(τ)
$\|a_0\|^2$	τ_0
$\|a_1\|^2$	τ_1
$\|a_2\|^2$	τ_2
$\|a_3\|^2$	τ_3

Power profile of the channel is given by equation 2.15.

$$\varphi(\tau) = |h(\tau)|^2$$

$$= \sum_{i=0}^{L-1} a_i^2 \delta(\tau - \tau_i)$$

$$= \sum_{i=0}^{L-1} g_i \delta(\tau - \tau_i) \qquad (2.15)$$

Hence we get multiple copies due to scattering. These copies are occurring over an interval of time [5]. This time interval is termed "delay spread," shown in Figure 2.4.

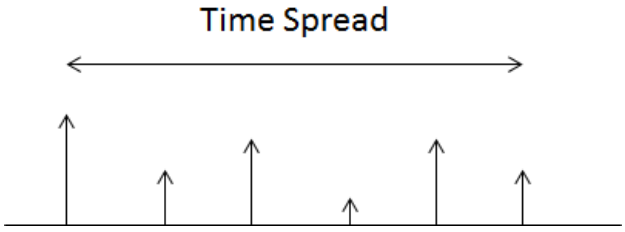

Figure 2.4: Delay spread.

2.3.1 Maximum Delay Spread

The first component of the signal arrives after a delay of τ_0 and the last component comes to the receiver at τ_{L-1}. The maximum delay spread is given by equation 2.16.

$$\sigma_{\tau max} = \tau_{L-1} - \tau_0 \qquad (2.16)$$

2.3.2 RMS Delay Spread

The signals received after a long time come with less power and these signals are not received by the receiver, which causes problem in calculating the delay spread. Hence root mean

square (RMS) delay spread is an effective way to overcome this problem because low-power paths are not considered in calculating delay spread in RMS delay spread.

Normalized fraction of power in the i^{th} path is given by equation 2.17 in which g_i is the power associated with the i^{th} multipath.

$$b_i = \frac{g_i}{g_0 + g_1 + \cdots + g_{L-1}}$$

$$b_i = \frac{g_i}{\sum_{j=0}^{L-1} g_j} \tag{2.17}$$

Average delay is given by equation 2.18.

$$\tau' = b_0\tau_0 + b_1\tau_1 + \cdots + b_{L-1}\tau_{L-1}$$

$$\tau' = \sum_{i=0}^{L-1} b_i\tau_i$$

$$\tau' = \sum_{i=0}^{L-1} \frac{g_i\tau_i}{\sum_{j=0}^{L-1} g_j} = \frac{\text{weighted delay}}{\text{total power}} \tag{2.18}$$

Using the value of average delay, the RMS delay spread can be calculated.

$$\sigma_\tau^2 = b_0(\tau_0 - \tau')^2 + b_1(\tau_1 - \tau')^2 + \cdots + b_{L-1}(\tau_{L-1} - \tau')^2$$

$$= \sum_{i=0}^{L-1} b_i(\tau_i - \tau')^2$$

$$= \sum_{i=0}^{L-1} \frac{g_i(\tau_i - \tau')^2}{\sum_{i=0}^{L-1} g_i}$$

$$\sigma_\tau = \sqrt{\sum_{i=0}^{L-1} \frac{g_i(\tau_i - \tau')^2}{\sum_{j=0}^{L-1} g_j}} \tag{2.19}$$

2.4 Coherence Bandwidth

Coherence bandwidth is a statistical measurement of the range of frequencies over which the channel can be considered "flat." The coherence bandwidth can be calculated by taking the Fourier transform of the channel delay profile. Considering the Fourier transform of the channel delay profile, a low pass sort of characteristics is observed. The frequency band stays constant or flat for some portion of the characteristics. The flat portion is termed as coherence bandwidth.

Figure2.5. shows the regular coherence bandwidth spectrum. B_c is the coherence bandwidth.

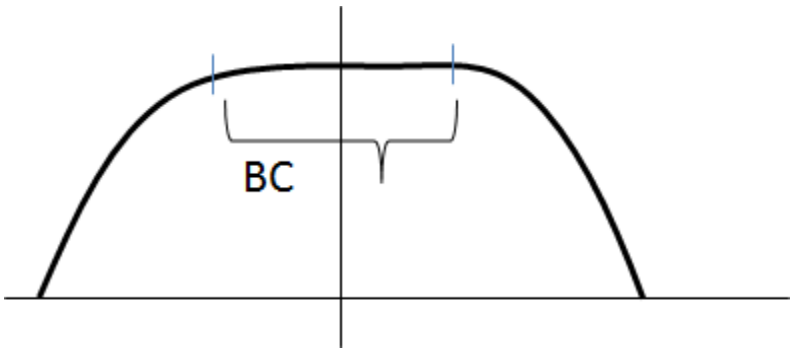

Figure 2.5: Coherence bandwidth spectrum.

If signal bandwidth is greater than the coherence bandwidth, the edges of input are attenuated due to which the output gets distorted. Such a phenomenon is known as frequency selective fading response. Equation 2.20 represents the Fourier transform of the channel.

$$H(f) = \sum a_i e^{-j2\pi f \tau_i} \qquad (2.20)$$

Mathematically, coherence bandwidth in terms of delay spread is given by equation 2.21.

$$B_c = \frac{1}{2\sigma_\tau} \qquad (2.21)$$

A channel can be called as frequency nonselective or flat fading channel if the bandwidth of the signal is less than or equal to the coherence bandwidth. Distortion is eliminated in this case. If bandwidth of the signal is greater than the coherence bandwidth, output is distorted because of the attenuated edges of input. This situation is called frequency selective fading response or inter-block interference (IBI) [5], a phenomenon where the delay spread is larger than symbol duration. In this case, the previous symbol interferes with the current symbol. If the delay spread is less than the symbol duration, the same symbol interferes with itself. This is why GSM is considered a frequency nonselective channel and 3G/4G is considered a frequency selective fading system. Loss of data at the receiver occurs due to ISI which reduces the performance of communication. Hence equalizers are used to make the frequency selective fading system a flat fading response.

2.5 Doppler Shift

Due to the relative motion between the transmitter and the receiver, there is a variation in the frequency of the electromagnetic (EM) wave. This phenomenon is known as Doppler effect. This change in frequency causes incorrect results in real-time communication systems. Hence, this has to be negated. Figure 2.6 shows the system which demonstrates Doppler effect.

Figure 2.6: Cause of Doppler effect.

2.5.1 Computation of Doppler Shift

Consider a situation where the MS is moving at an angle θ with respect to the BS as shown in Figure 2.7.

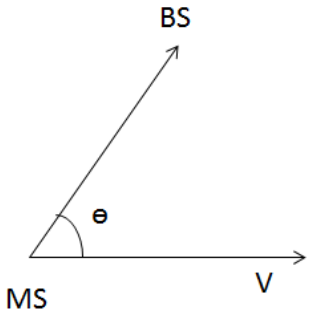

Figure 2.7: Motion of BS.

The received frequency f_r is now equal to the sum of carrier frequency f_c and the Doppler frequency f_d as shown in equation 2.22.

$$f_d = \frac{V\cos\theta}{c} * f_c$$

$$f_r = f_c + f_d = f_c + \frac{V\cos\theta}{c} * f_c \qquad (2.22)$$

$0 \leq \theta \leq \frac{\pi}{2}$: The MS is moving towards the BS

$\frac{\pi}{2} \leq \theta \leq \pi$: The MS is moving away from the BS

For any other condition, even though the MS has a velocity, there is no effect of Doppler on the system whatsoever. For typical values of f_c = 1850 MHz, V = 60 mph towards BS, the computed Doppler shift is about 165 Hz. The received frequency is therefore 1850 MHz + 165 Hz. This value may look small, but it has a huge impact.

2.5.2 Effect on Channel

If a_i represents the attenuation of ith path and τ_i represents the delay of the ith path, then the baseband channel can be denoted as $a_i\delta(t-\tau_i)$. The delay in this path is decreased by $\tau_i - \frac{Vt}{c}$ since the distance between the MS and the BS is decreased by Vt on increasing time t. Here, MS is moving at an angle θ with respect to BS; therefore, delay in this case becomes $\tau_i - \frac{Vcos\theta t}{c}$.

The flat fading channel coefficient as discussed previously is given as

$$h = \sum_{i=0}^{L-1} a_i e^{-j2\pi f_c \tau_i}$$

Since MS is moving with respect to BS, it becomes the function of t. Therefore equation2.23 gives new flat fading coefficient.

$$h(t) = \sum_{i=0}^{L-1} a_i\, e^{-j2\pi f_c \tau_i(t)} \tag{2.23}$$

While using the delay value which is obtained from theoretical analysis,

$$h(t) = \sum_{i=0}^{L-1} a_i\, e^{-j2\pi f_c\left(\tau_i - \frac{Vcos\theta t}{c}\right)} \tag{2.24}$$

The new flat fading coefficient can be divided into two different random variables.

$$h(t) = \sum_{i=0}^{L-1} a_i e^{-j2\pi f_c \tau_i}\; e^{j2\pi f_c\left(\frac{vcos\theta t}{c}\right)}$$

$$h(t) = \sum_{i=0}^{L-1} a_i e^{-j2\pi f_c \tau_i}\; e^{j2\pi f_d t} \tag{2.25}$$

The Doppler term f_d in the above equation leads to time-varying phase. Now Doppler has become a time-selective channel. At this point of time, a parameter called coherence time T_c can be determined. T_c is the time where the channel remains constant [5]. The channel has to be measured once every coherence time to understand the channel because the coherence time is approximately 1ms in active wireless applications. Coherence time is measured mathematically where it is equal to reciprocal of four times the maximum Doppler shift.

2.5.3 Doppler Spectrum

Doppler is calculated using a correlation function of the channel. Correlation is the measure of similarity or dissimilarity. The higher the correlation between the two variables, the more similar they are. If X and Y are considered as two random variables, then the correlation between X and Y is mathematically represented as E{XY*}.

$$a_i(t) = a_i e^{-j2\pi f \tau_i} e^{j2\pi f_d t}$$

If $E\{a_i(t) * a_i^*(t+\Delta t)\}$ is high, then the channel hasn't changed.

$$a_i(t+\Delta t) = a_i e^{-j2\pi f \tau_i} e^{j2\pi f_d (t+\Delta t)}$$

$$\psi(\Delta t) = E\{|a_i|^2 e^{-j2\pi f_d \Delta t}\}$$

$$\psi(\Delta t) = E\{a_i(t+\Delta t)\}$$

Normalizing $|a_i|^2 = 1$, we get the equation 2.26.

$$\psi(\Delta t) = E\left\{e^{-j2\pi f_d \Delta t}\right\} \quad (2.26)$$

This is known as the correlation coefficient. Substituting the value of Doppler frequency we get

$$\psi(\Delta t) = E\left\{e^{-\frac{j2\pi f_c V}{c} cos\theta \Delta t}\right\} \quad (2.27)$$

We know that $f_{dmax} = \frac{f_c V}{c}$ $when\ \theta = 0$. Therefore the equation 2.27 becomes equation 2.28.

$$\psi(\Delta t) = E\left\{e^{-j2\pi f_{dmax}\cos\theta\,\Delta t}\right\} \tag{2.28}$$

Assuming that θ is uniformly distributed between 0 and π, we get equation 2.29.

$$\psi(\Delta t) = \int_0^{\pi} \frac{1}{\pi} e^{-j2\pi f_{dmax}\Delta t\cos\theta}\, d\theta \tag{2.29}$$

The solution for equation 2.29 is in terms of the Bessel function and it is as follows:

$$\psi(\Delta t) = J_0(2\pi f_{dmax}\Delta t)$$

Here J_0 is the Bessel function of 0^{th} order [5]. The above expression can also be written as

$$\psi(\Delta t) = J_0\left(\frac{2\pi\Delta t}{4T_c}\right) = J_0\left(\frac{\pi}{2} * \frac{\Delta t}{T_c}\right) \tag{2.30}$$

In practical applications, any correlation below 0.5 is considered as a change in channel parameters [5]. Finally, the Doppler spectrum is nothing but the Fourier transform of the autocorrelation function [5], i.e., equation 2.30, which is given as follows:

$$S_H(f) = \int_{-\infty}^{\infty} \psi(\Delta t) e^{-j2\pi f\Delta t}\, d(\Delta t)$$

$$S_H(f) = \int_{-\infty}^{\infty} J_0(2\pi f_{dmax}\Delta t) e^{-j2\pi f\Delta t}\, d(\Delta t)$$

$$S_H(f) = \frac{\frac{1}{\pi f_{dmax}}\,\mathrm{rect}\left(\frac{f}{f_d}\right)}{\sqrt{1-\left(\frac{f}{f_d}\right)^2}} \tag{2.31}$$

Equation 2.31 represents the Doppler spectrum. The plot of the above spectrum is shown in Figure 2.8. It is evident from the plot that the Doppler spectrum exists only between the intervals $-f_d$ to f_d. The spectrum shown in Figure 2.8 is also known as U-shaped spectrum or Jake's spectrum or Jake's model.

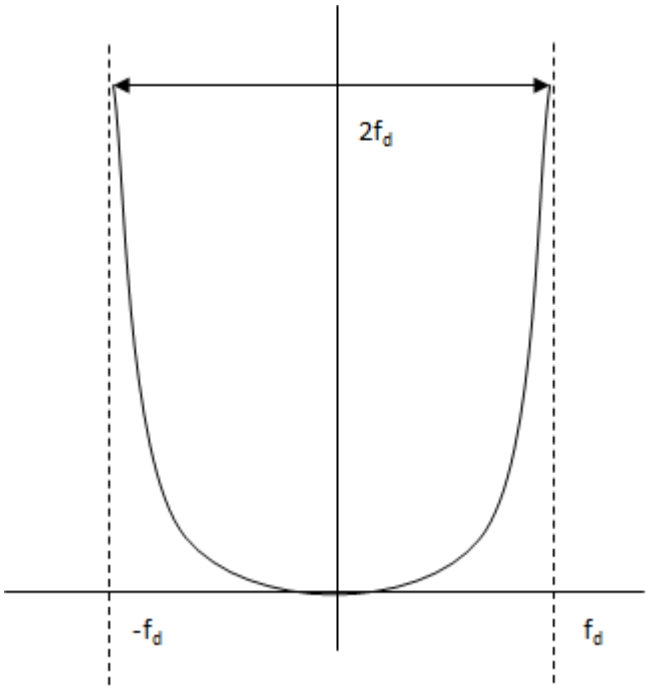

Figure 2.8: Jake's spectrum [5].

CHAPTER 3: MULTICARRIER MODULATION AND OFDM

3.1 Multicarrier Modulation

In single-carrier modulation technique one carrier occupies the entire bandwidth. If 'B' is the bandwidth available for communication, the symbol duration will be $T = 1/B$. One symbol is transmitted every T seconds. It is typically two symbols as there is a 'sine' and a 'cosine' term associated with a signal. Symbol rate is the inverse of transmission time which is equal to B. If the available bandwidth is divided into 'N' subcarriers and each data symbol is modulated with the individual subcarrier, the system becomes a multicarrier system. The bandwidth of each subcarrier is $f_n = B/N$ and consequently the spacing between each subcarrier [6]. A typical multicarrier spectrum is shown in Figure 3.1.

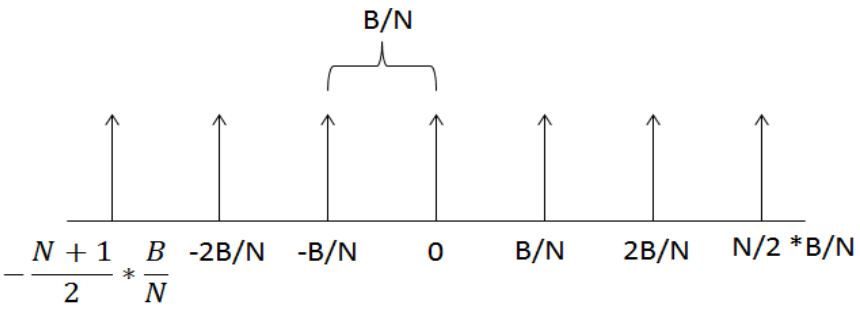

Figure 3.1: Subcarrier spacing.

3.1.1 Transmission

In multicarrier transmission, the center frequency of the i^{th} subcarrier is given by equation 3.1.

$$f_i = \frac{iB}{N} \tag{3.1}$$

X_i is the data to be transmitted on the i^{th} subcarrier. The modulated data stream is given by equation 3.2.

$$S_i(t) = X_i e^{j2\pi f_i t} \tag{3.2}$$

In a multicarrier system, there are a total of N subcarriers. Hence, N data symbols can be modulated using the N subcarriers. Before transmitting, the N modulated streams are added. The composite transmit signal is given by equation 3.3 [6].

$$S(t) = \sum_i X_i e^{\frac{j2\pi iB}{N}t} \tag{3.3}$$

Figure 3.2 clearly shows the block diagram to implement a multicarrier system.

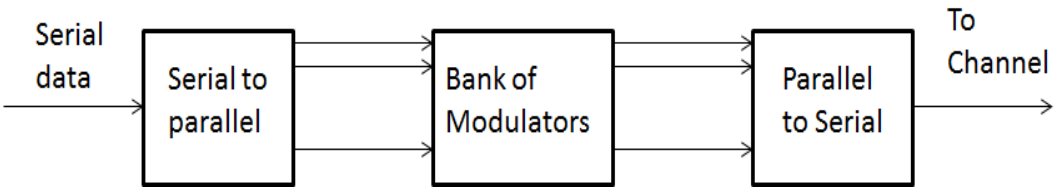

Figure 3.2: Block diagram of multicarrier transmitter system [6].

3.1.2 Reception

At the receiver, the received signal is the transmitted signal combined with noise. Ignoring the effect of noise, the received signal is the same as the composite transmitted signal given by equation 3.3. To get back the original data symbols, each stream is coherently demodulated with its corresponding subcarrier [6]. The process of correlation is done with the l^{th} subcarrier.

$$= \frac{B}{N}\int_0^{\frac{N}{B}} \sum_i X_i e^{\frac{j2\pi iB}{N}t} e^{-\frac{j2\pi lB}{N}t} dt$$

$$= \frac{B}{N}\sum_i \int_0^{\frac{N}{B}} \frac{X_i e^{\frac{j\pi(i-l)B}{N}t} B}{N} t\, dt$$

$$\int_0^{\frac{N}{B}} e^{\frac{j2\pi(i-l)B}{N}t} = \begin{cases} 0 & \text{if } i \neq l \\ \frac{N}{B} & \text{if } i = l \end{cases}$$

All subcarriers except l^{th} subcarrier are orthogonal to the l^{th} subcarrier. Hence we can correlate with $e^{-j2\pi f_l t}$. After demodulation with l^{th} coherent subcarrier, we get back the original data stream [6]. The block diagram of an MCM receiver is shown in Figure 3.3.

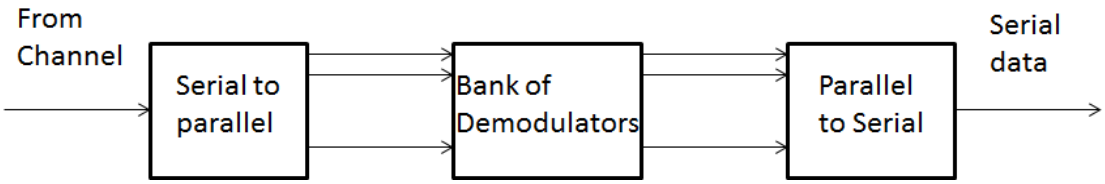

Figure 3.3: Block diagram of multicarrier receiver System [6].

The window of time associated with detection of this multicarrier signal is N/B, which is the time period of integration [6]. Hence, multicarrier modulation transmits N symbols using N subcarriers in time period N/B. The symbol rate is N/(N/B) = B. The net symbol rate using single-carrier vs. multicarrier modulation has not changed. Therefore, nothing has been achieved in terms of symbol rate [6].

3.2 OFDM

Implementing N bank of modulators or correlators and demodulators or decorrelators is a very difficult task as it leads to phase offsets and also increases the cost required to install 2N oscillators [6]. However, there was a key advancement made by Weinstein and Ebert in 1971 at

Bell Labs [7]. The Nyquist sampling rate of a multicarrier system is B. The multicarrier system is band limited to B. Consider the u^{th} sample in the system which is given by equation 3.4.

$$S(uT_s) = x(u) = \sum_i X_i e^{\frac{j2\pi iB}{N}\frac{U}{B}} = \sum_i X_i e^{\frac{j2\pi iU}{N}} \quad (3.4)$$

From equation 3.4, it is evident that the output samples are the IDFT of the information symbols. This theory formulated by Weinstein and Ebert provided a breakthrough in modeling the OFDM system. The IDFT and DFT operations replace the modulators and demodulators, making it very efficient. In practice, the IDFT and DFT are implemented by IFFT and FFT operations in the digital signal processor. This proposed scheme of generating the multicarrier transmit signal has a much lower implementation complexity compared to the bank of correlators [6]. Such a system is termed as OFDM. The name orthogonality is used as OFDM uses orthogonal subcarriers instead of random subcarrier frequencies, making it much easier to demodulate on the receiver due to the orthogonality principle.

The coherence bandwidth in outdoor channels for a 3G/4G system is about 300 kHz. The bandwidth for an OFDM system is about 2 GHz. It can be clearly seen that bandwidth is very much higher than the coherence bandwidth. This leads to inter-symbol interference (ISI). OFDM employs smart methods to combat the issue of ISI or IBI.

3.2.1 Transmitter

The block schematic of an OFDM transmitter is demonstrated in Figure 3.4. The raw data bits are modulated using various digital modulation schemes like QAM, PSK and BPSK. Since OFDM focuses on parallel transmission of data, the serial data after modulation is converted into parallel data. The size of the parallel data depends upon the number of subcarriers used. The

parallel symbol stream is then sent to the modulator block, which is now replaced by the IFFT operation. Here, each data symbol is modulated with its corresponding subcarrier. The parallel modulated data is now converted into serial data and it goes into the cyclic prefix module. In this block, the last few symbols are copied and attached at the beginning of the OFDM symbol. This is done mainly to avoid the effects of multipath propagation and fading. After the addition of cyclic prefix, the data is sent out into the channel which is to be captured by the receiver.

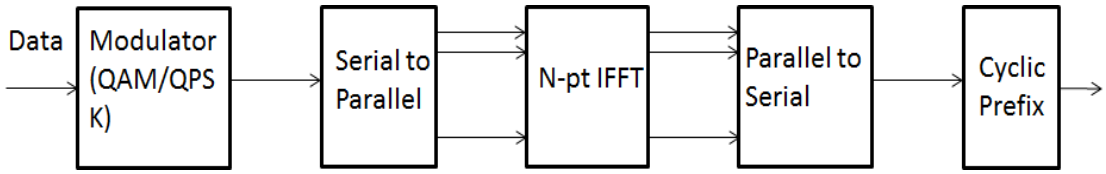

Figure 3.4: OFDM transmitter block diagram [6].

N represents the number of subcarriers. Typically the number of subcarriers is a power of 2. In practical applications, the number of subcarriers is equal to $2^x * 3^y * 5^z$, where x, y and z's are integers.

3.2.2 Receiver

At the receiver, the opposite procedure is done compared to the transmitter. The symbols received are first deprived of the cyclic prefix. The serial symbol stream is converted into a parallel symbol stream by using the multiplexer or serial to parallel converter. The parallel symbol stream is demodulated by using the N-pt FFT operation. FFT is a correlator or a frequency domain sampler. The parallel symbol stream after the FFT operation is demodulated to the baseband and serialized, which goes to various applications. Figure 3.5 shows the schematic block diagram of a typical OFDM receiver.

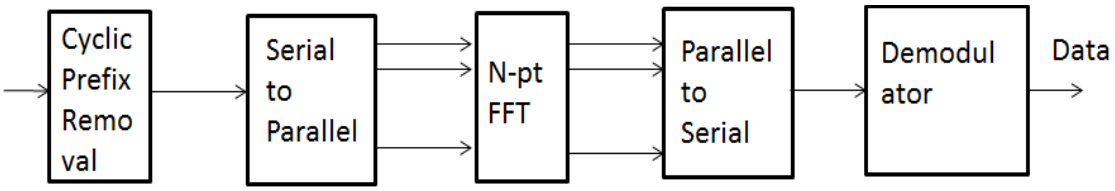

Figure 3.5: OFDM receiver block diagram [6].

CHAPTER 4: MIMO STBC AND INTRODUCTION TO ALAMOUTI CODING

4.1 Introduction to MIMO

MIMO system is the use of multiple antennas both at transmitter and receiver to enhance communication performance. MIMO technology combined with OFDM and space-time block coding represents an interesting candidate for mobile communication due to its ability to withstand high speeds, high capacity and robustness to multipath fading. In the scenario, where mobility is required for the data transmission, MIMO-OFDM is deployed for transmit diversity and secure means for data propagation.

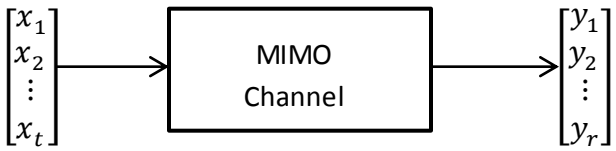

$$\begin{bmatrix} y_1 \\ y_2 \\ \vdots \\ y_r \end{bmatrix}_{rX1} = \begin{bmatrix} h_{11} & h_{12} & \cdots & h_{1t} \\ h_{21} & h_{22} & \cdots & h_{2t} \\ \vdots & \vdots & \ddots & \vdots \\ h_{r1} & h_{r2} & \cdots & h_{rt} \end{bmatrix}_{rXt} \begin{bmatrix} x_1 \\ x_2 \\ \vdots \\ x_t \end{bmatrix}_{tX1} \tag{4.1}$$

$$y_1 = h_{11}x_1 + h_{12}x_2 + \cdots + h_{1t}x_t \tag{4.2}$$

$$y_2 = h_{21}x_1 + h_{22}x_2 + \cdots + h_{2t}x_t \tag{4.3}$$

MIMO channel matrix is given by

$$H = \begin{bmatrix} h_{11} & h_{12} & \cdots & h_{1t} \\ h_{21} & h_{22} & \cdots & h_{2t} \\ \vdots & \vdots & \ddots & \vdots \\ h_{r1} & h_{r2} & \cdots & h_{rt} \end{bmatrix}_{rXt} \tag{4.4}$$

MIMO system model

$$\begin{bmatrix} y_1 \\ y_2 \\ \vdots \\ y_r \end{bmatrix}_{rX1} = \begin{bmatrix} h_{11} & h_{12} & \cdots & h_{1t} \\ h_{21} & h_{22} & \cdots & h_{2t} \\ \vdots & \vdots & \ddots & \vdots \\ h_{r1} & h_{r2} & \cdots & h_{rt} \end{bmatrix}_{rXt} \begin{bmatrix} x_1 \\ x_2 \\ \vdots \\ x_t \end{bmatrix}_{tX1} + \begin{bmatrix} n_1 \\ n_2 \\ \vdots \\ n_r \end{bmatrix}_{rX1} \tag{4.5}$$

$$\bar{y}_{rX1} = H_{rXt}\bar{x}_{tX1} + \bar{n}_{rX1} \tag{4.6}$$

Special Cases

t = 1:

$$\begin{bmatrix} y_1 \\ y_2 \\ \vdots \\ y_r \end{bmatrix} = \begin{bmatrix} h_{11} \\ h_{21} \\ \vdots \\ h_{r1} \end{bmatrix} x + \begin{bmatrix} n_1 \\ n_2 \\ \vdots \\ n_r \end{bmatrix}_{rX1} \tag{4.7}$$

This is known as receive diversity or SIMO (single input multiple output) system.

r=1:

$$y = [h_1 \quad h_2 \quad \ldots \quad h_t] \begin{bmatrix} x_1 \\ x_2 \\ \vdots \\ x_t \end{bmatrix} + n \tag{4.8}$$

$$\bar{y} = \bar{h}^T\bar{x} + n \tag{4.9}$$

This is known as transmit diversity or MISO (multiple input single output) system.

r = t= 1:

$$y = hx + n \tag{4.10}$$

This is known as SISO system (single input single output system).

Noise -$\bar{n}$:

$$\bar{n} = \begin{bmatrix} n_1 \\ n_2 \\ \vdots \\ n_r \end{bmatrix} \tag{4.11}$$

$$E[|n_i|^2] = \sigma_n^2 \tag{4.11}$$

$$\mathrm{E}\left[\mathrm{n_i}.\mathrm{n_j^*}\right] = 0 \tag{4.12}$$

$$\mathrm{R_n} = \mathrm{E}[\bar{\mathrm{n}}.\bar{\mathrm{n}}^{\mathrm{H}}] = \mathrm{E}\left(\begin{bmatrix} \mathrm{n}_1 \\ \mathrm{n}_2 \\ \vdots \\ \mathrm{n}_\mathrm{r} \end{bmatrix} [\mathrm{n}_1^* \quad \mathrm{n}_2^* \quad \ldots \quad \mathrm{n}_\mathrm{r}^*]\right) \tag{4.13}$$

$$= E\begin{bmatrix} |\mathrm{n}_1|^2 & \mathrm{n}_1\mathrm{n}_2^* & \ldots & \mathrm{n}_1\mathrm{n}_\mathrm{r}^* \\ \mathrm{n}_2\mathrm{n}_1^* & |\mathrm{n}_2|^2 & \ldots & \mathrm{n}_2\mathrm{n}_\mathrm{r}^* \\ \vdots & \vdots & \ddots & \vdots \\ \mathrm{n}_\mathrm{r}\mathrm{n}_1^* & \mathrm{n}_\mathrm{r}\mathrm{n}_2^* & \ldots & |\mathrm{n}_\mathrm{r}|^2 \end{bmatrix}$$

$$= \begin{bmatrix} \mathrm{E}|\mathrm{n}_1|^2 & \mathrm{E}(\mathrm{n}_1\mathrm{n}_2^*) & \ldots & \mathrm{E}(\mathrm{n}_1\mathrm{n}_\mathrm{r}^*) \\ \mathrm{E}(\mathrm{n}_2\mathrm{n}_1^*) & \mathrm{E}|\mathrm{n}_2|^2 & \ldots & \mathrm{E}(\mathrm{n}_2\mathrm{n}_\mathrm{r}^*) \\ \vdots & \vdots & \ddots & \vdots \\ \mathrm{E}(\mathrm{n}_\mathrm{r}\mathrm{n}_1^*) & \mathrm{E}(\mathrm{n}_\mathrm{r}\mathrm{n}_2^*) & \ldots & \mathrm{E}|\mathrm{n}_\mathrm{r}|^2 \end{bmatrix}$$

$$\begin{bmatrix} \sigma_\mathrm{n}^2 & 0 & \ldots & 0 \\ 0 & \sigma_\mathrm{n}^2 & \ldots & 0 \\ \vdots & \vdots & \ddots & \vdots \\ 0 & 0 & \ldots & \sigma_\mathrm{n}^2 \end{bmatrix}_{\mathrm{rXr}} = \sigma_\mathrm{n}^2 \mathrm{I}_{\mathrm{rXr}} \tag{4.14}$$

Noise is uncorrelated across antennas and time.

4.2 MIMO Receiver

4.2.1 Linear Receiver

At receiver

$$\mathrm{Y} = \mathrm{H}\,\mathrm{x} + \mathrm{n} \tag{4.17}$$

$$\mathrm{H}^{-1}Y = x + \mathrm{H}^{-1}n \tag{4.18}$$

Inverse exists for only r =t.

Generalized inverse $(r \geq t)$

$$\begin{bmatrix} y_1 \\ y_2 \\ \vdots \\ y_r \end{bmatrix}_{rX1} = \begin{bmatrix} h_{11} & h_{12} & \cdots & h_{1t} \\ h_{21} & h_{22} & \cdots & h_{2t} \\ \vdots & \vdots & \ddots & \vdots \\ h_{r1} & h_{r2} & \cdots & h_{rt} \end{bmatrix}_{rXt} \begin{bmatrix} x_1 \\ x_2 \\ \vdots \\ x_t \end{bmatrix}_{tX1} + \begin{bmatrix} n_1 \\ n_2 \\ \vdots \\ n_r \end{bmatrix}_{rX1} \tag{4.19}$$

$$\text{Error} = \left|\left|y - Hx\right|\right|^2 \tag{4.20}$$

Vector differentiation:

$$\bar{x} = \begin{bmatrix} x_1 \\ x_2 \\ \vdots \\ x_t \end{bmatrix} \tag{4.21}$$

$$\frac{df}{d\bar{x}} = \begin{bmatrix} \frac{df}{dx_1} \\ \frac{df}{dx_2} \\ \vdots \\ \frac{df}{dx_t} \end{bmatrix} \tag{4.22}$$

Let

$$f(\bar{x}) = \bar{C}^T\bar{x} = \bar{x}^T\bar{C} = C_1x_1 + C_2x_2 + \cdots + C_tx_t \tag{4.23}$$

$$\frac{d(\bar{C}^T\bar{x})}{d\bar{x}} = \begin{bmatrix} C_1 \\ C_2 \\ \vdots \\ C_t \end{bmatrix} = \bar{C} \tag{4.24}$$

$$\frac{d(\bar{C}^T\bar{x})}{d\bar{x}} = \frac{d(\bar{x}^T\bar{C})}{d\bar{x}} = \bar{C} \tag{4.25}$$

Now go back to error

$$\text{Error} = \left|\left|y - Hx\right|\right|^2 \tag{4.26}$$

$$= (y - Hx)^T(y - Hx)$$

$$= \bar{y}^T\bar{y} - \bar{x}H^T\bar{y} - \bar{y}^TH\bar{x} + \bar{x}H^TH\bar{x}$$

Differentiating with respect to x

$$0 - \mathrm{H}^{\mathrm{T}}\bar{\mathrm{y}} - \mathrm{H}^{\mathrm{T}}\bar{\mathrm{y}} + \mathrm{H}^{\mathrm{T}}\mathrm{H}\bar{\mathrm{x}} + \mathrm{H}^{\mathrm{T}}\mathrm{H}\bar{x}$$

$$\frac{\mathrm{d}\left|\left|\bar{\mathrm{y}} - \mathrm{H}\bar{\mathrm{x}}\right|\right|^{2}}{\mathrm{dx}} = -2\mathrm{H}^{\mathrm{T}}\bar{\mathrm{y}} + 2\mathrm{H}^{\mathrm{T}}\mathrm{H}\bar{\mathrm{x}} \tag{4.27}$$

For optimal value $-2H^T\bar{y} + 2H^T H\bar{x} = 0$

$$H^T H\bar{x} = H^T\bar{y}$$

$$\bar{x} = (H^T H)^{-1}H^T\bar{y} \tag{4.28}$$

This solution is known as zero forcing receivers.

Diversity of zero forcing receivers = **r-t+1.**

4.2.2 MIMO MMSE Receiver

$$\bar{y} = \begin{bmatrix} y_1 \\ y_2 \\ \vdots \\ y_r \end{bmatrix} \longrightarrow r\ measurements$$

Linear estimator: $\hat{x} = \bar{C}^T\bar{y}$

Choose $\bar{C}$ such that

$$\mathrm{E}\left[\left|\left|\bar{\mathrm{x}} - \mathrm{x}\right|\right|^{2}\right] = \mathrm{E}\left[\left|\left|\bar{\mathrm{C}}^{\mathrm{T}}\bar{\mathrm{y}} - \mathrm{x}\right|\right|^{2}\right] \tag{4.29}$$

$$= (\bar{\mathrm{C}}^{\mathrm{T}}\bar{\mathrm{y}} - \mathrm{x})^{\mathrm{T}}(\bar{\mathrm{C}}^{\mathrm{T}}\bar{\mathrm{y}} - \mathrm{x})$$

$$= \mathrm{C}^{\mathrm{T}}\bar{\mathrm{y}}\bar{\mathrm{y}}^{\mathrm{T}}\bar{\mathrm{C}} - \mathrm{x}\bar{\mathrm{y}}^{\mathrm{T}}\bar{\mathrm{C}} - \bar{\mathrm{C}}^{\mathrm{T}}\bar{\mathrm{y}}\mathrm{x} + \mathrm{x}\mathrm{x}^{\mathrm{T}}$$

$$\mathrm{E}(\bar{\mathrm{y}}\bar{\mathrm{y}}^{\mathrm{T}}) = \mathrm{R}_{\mathrm{yy}} \tag{4.30}$$

$$\mathrm{E}(\mathrm{x}\bar{\mathrm{y}}^{\mathrm{T}}) = \mathrm{R}_{\mathrm{xy}} \tag{4.31}$$

$$\mathrm{E}(\mathrm{y}\mathrm{x}^{\mathrm{T}}) = \mathrm{R}_{\mathrm{xy}}^{\mathrm{T}} = \mathrm{R}_{\mathrm{yx}} \tag{4.32}$$

$$= \mathrm{C}^{\mathrm{T}}\mathrm{R}_{\mathrm{yy}}\bar{\mathrm{C}} - \mathrm{R}_{\mathrm{xy}}\bar{\mathrm{C}} - \bar{\mathrm{C}}^{\mathrm{T}}\mathrm{R}_{\mathrm{yx}} + \mathrm{R}_{\mathrm{xx}}$$

$$E\left[\left||\bar{C}^T\bar{y}-x|\right|^2\right]=\bar{C}^T R_{yy}\bar{C}-2\bar{C}^T R_{yx}+R_{xx} \tag{4.33}$$

$\frac{\partial f}{\partial \bar{C}}=0$ For minimum

$$\frac{\partial f(\bar{C})}{\partial \bar{C}}=2R_{yy}\bar{C}-2R_{yx}=0 \tag{4.34}$$

$$R_{yy}\bar{C}=R_{yx} \tag{4.35}$$

$$\bar{C}=R_{yy}^{-1}R_{yx} \tag{4.36}$$

LMMSE for complex vectors is $\hat{x}=\bar{C}^H\bar{y}$.

MIMO system model $\bar{y}=H\bar{x}+\bar{n}$

$$E\{x\bar{x}^H\}=\text{covariance of transmitted symbols}=R_{xx}$$

$$R_{xx}=E\left\{\begin{bmatrix}x_1\\x_2\\\vdots\\x_t\end{bmatrix}\begin{bmatrix}x_1^* & x_2^* & \dots & x_t^*\end{bmatrix}\right\}=E\begin{bmatrix}|x_1|^2 & x_1x_2^* & \dots & x_1x_t^*\\x_2x_1^* & |x_2|^2 & \dots & x_2x_t^*\\\vdots & \vdots & \ddots & \vdots\\x_tx_1^* & x_tx_2^* & \dots & x_t^2\end{bmatrix}_{tXt} \tag{4.37}$$

$$=\begin{bmatrix}P_d & 0 & \dots & 0\\0 & P_d & \dots & 0\\\vdots & \vdots & \ddots & \vdots\\0 & 0 & \dots & P_d\end{bmatrix}_{tXt}$$

$$R_{xx}=P_d.I_{tXt} \tag{4.38}$$

$$R_{yy}=E\{y\bar{y}^H\}=E\{(H\bar{x}+\bar{n})(H\bar{x}+\bar{n})^H\} \tag{4.39}$$

$$=E\{(H\bar{x}\bar{x}^HH^H+\bar{n}\bar{n}^H)\}$$

$$=HR_{xx}H^H+\sigma_n^2I$$

$$R_{yy}=P_dHH^H+\sigma_n^2I \tag{4.40}$$

$$R_{yx}=E\{\bar{y}\bar{x}^H\}=E\{(H\bar{x}+\bar{n})\bar{x}^H\} \tag{4.41}$$

$$=E\{H\bar{x}\bar{x}^H+\bar{n}\bar{x}^H\}$$

$$=E\{H\bar{x}\bar{x}^H\}$$

$$= P_d H$$

$$\bar{C} = R_{yy}^{-1} R_{yx} \tag{4.42}$$

$$= (P_d H H^H + \sigma_n^2 I)^{-1} P_d H$$

$$= P_d (P_d H H^H + \sigma_n^2 I)^{-1} H$$

$$\hat{x} = \bar{C}^H \bar{y} \tag{4.43}$$

$$\hat{x} = P_d H^H (P_d H H^H + \sigma^2 I) H^H y \tag{4.44}$$

For single receiver and transmitter, H = h.

$$\hat{x} = P_d \left(\frac{h^*}{P_d |h|^2 + \sigma_n^2} \right) \bar{y} \tag{4.45}$$

$$\hat{x} = \frac{P_d h^*}{\sigma_n^2} \tag{4.46}$$

If |h| = 0, MIMO doesn't blow noise.

We know

$$\hat{x}_{MMSE} = P_d (P_d H^H H + \sigma_n^2) H^H \bar{y} \tag{4.47}$$

At high SNR,

$$\hat{x}_{MMSE} \cong P_d (P_d H^H H)^{-1} H^H \bar{y} \tag{4.48}$$

$$\cong (H^H H)^{-1} H^H \bar{y}$$

$$\hat{x}_{MMSE} \cong P_d (\sigma_n^2 I)^{-1} H^H \bar{y}$$

$$\hat{x}_{MMSE} = \frac{P_d}{\sigma_n^2} H^H \bar{y} \tag{4.49}$$

Decomposition of MIMO channel:

$$H = u \varepsilon V^H \tag{4.50}$$

$$= \begin{bmatrix} u_1 & u_2 & \cdots & u_t \\ \vdots & \vdots & \vdots & \vdots \end{bmatrix}_{rXt} \begin{bmatrix} \sigma_1 & 0 & \dots & 0 \\ 0 & \sigma_2 & \dots & 0 \\ \vdots & \vdots & \ddots & \vdots \\ 0 & 0 & \dots & \sigma_t \end{bmatrix}_{tXt} \begin{bmatrix} V_1^H & \dots \\ V_2^H & \dots \\ \vdots & \dots \\ V_t^H & \dots \end{bmatrix}_{tXt}$$

$$\left||u_i|\right|^2 = 1 \qquad u_1^H u_j = 0 \qquad \text{if } i \neq j$$

$$\left||V_i|\right|^2 = 1 \qquad V_1^H V_j = 0 \qquad \text{if } i \neq j$$

$V^H V = VV^H = I$ V is a unitary matrix

$\sigma_1, \sigma_2 \dots \sigma_t$ are known as singular values.

$$\sigma_1, \sigma_2 \dots \sigma_t \geq 0 \tag{4.51}$$

$\sigma_1 \geq \sigma_2 \geq \sigma_3 \geq \cdots \sigma_t \geq 0$. Singular values are ordered.

Number of nonsingular values is equal to the rank of the matrix. From equation (4.17),

$$\bar{y} = H\bar{x} + \bar{n}$$

$$\bar{y} = u\varepsilon V^H + \bar{n} \tag{4.52}$$

At the receiver, multiply $\bar{y}$ with u^H:

$$uy = \bar{y} = u^H(u\varepsilon V\bar{x} + \bar{n}) \tag{4.53}$$

$$\tilde{y} = \varepsilon V\bar{x} + u^H\bar{n}$$

$$\tilde{y} = \varepsilon V\bar{x} + \tilde{n} \tag{4.54}$$

At transmitter, $\bar{x} = \tilde{x}V^H$.

$$\tilde{y} = \varepsilon VV^H\tilde{x} + \tilde{n} \tag{4.55}$$

$$\tilde{y} = \varepsilon\tilde{x} + \tilde{n} \tag{4.56}$$

Decoupling of MIMO system (parallelization of MIMO system):

$$\begin{bmatrix}\widetilde{y_1}\\ \widetilde{y_2}\\ \vdots\\ \widetilde{y_t}\end{bmatrix}=\begin{bmatrix}\sigma_1 & 0 & \dots & 0\\ 0 & \sigma_2 & \dots & 0\\ \vdots & \vdots & \ddots & \vdots\\ 0 & 0 & \dots & \sigma_t\end{bmatrix}\begin{bmatrix}\widetilde{x_1}\\ \widetilde{x_2}\\ \vdots\\ \widetilde{x_t}\end{bmatrix}+\begin{bmatrix}\widetilde{n_1}\\ \widetilde{n_2}\\ \vdots\\ \widetilde{n_t}\end{bmatrix} \tag{4.57}$$

$$\begin{aligned}\widetilde{y_1}&=\sigma_1\widetilde{x_1}+\widetilde{n_1}\\ \widetilde{y_2}&=\sigma_2\widetilde{x_2}+\widetilde{n_2}\\ &\vdots\\ \widetilde{y_t}&=\sigma_t\widetilde{x_t}+\widetilde{n_t}\end{aligned} \tag{4.58}$$

This is called spatial multiplexing.

$$\tilde{n}=u^H n \tag{4.59}$$

$$E\{\tilde{n}\tilde{n}^H\}=E\{u^H n n^H u\} \tag{4.60}$$

$$=u^H\sigma_n^2 I u$$

$$=\sigma_n^2 u^H u$$

$$=\sigma_n^2 I_{tXt} \tag{4.61}$$

SNR of i-th parallel path $=\frac{\sigma_i^2 P_i}{\sigma_n^2}$.

Maximum rate = Shannon capacity = $\log_2(1+\text{SNR})$. (4.62)

So for i-th path = $\log_2\left(1+\frac{P_i\sigma_i^2}{\sigma_n^2}\right)=$ Capacity of i^{th} channel, total MIMO capacity

$$\sum_{i=1}^{t}\log_2\left(1+\frac{P_i\sigma_i^2}{\sigma_n^2}\right) \tag{4.63}$$

Optimal allocation of power 'P' to all transmitted streams:

$$P_1+P_2+\cdots+P_t\le P \tag{4.64}$$

Maximizing capacity:

$$\max\sum_{i=1}^{t}\log_2\left(1+\frac{P_i\sigma_i^2}{\sigma_n^2}\right) \tag{4.65}$$

Constraint:

$$\sum_{i=1}^{t}P_i\le P_{total} \tag{4.66}$$

$$f = \sum_{i=1}^{t} \log_2\left(1 + \frac{P_i \sigma_i^2}{\sigma_n^2}\right) + \lambda(P - \varepsilon P_i) \tag{4.67}$$

To maximize the capacity, $\frac{df}{dP_i} = 0$

$$\frac{\frac{\sigma_1^2}{\sigma_n^2}}{1+\frac{P_i \sigma_i^2}{\sigma_n^2}} + \lambda(-1) = 0 \tag{4.68}$$

$$\frac{\sigma_1^2}{\sigma_n^2} = \lambda\left(1 + \frac{P_i \sigma_i^2}{\sigma_n^2}\right) \tag{4.69}$$

$$\frac{1}{\lambda} = \frac{\sigma_n^2}{\sigma_i^2} + P_i \tag{4.70}$$

$$P_i = \left(\frac{1}{\lambda} - \frac{\sigma_n^2}{\sigma_i^2}\right)^* \tag{4.71}$$

$$\sum_{i=1}^{t} P_i \leq P \tag{4.72}$$

$$\sum_{i=1}^{t} \left(\frac{1}{\lambda} - \frac{\sigma_n^2}{\sigma_1^2}\right)^* = P \tag{4.73}$$

$$\frac{1}{\lambda} \geq \frac{\sigma_n^2}{\sigma_i^2} \text{ for all } i = 1,2,3,\ldots,N$$

$$P = \sum_{i=1}^{t} \left(\frac{1}{\lambda} - \frac{\sigma_n^2}{\sigma_i^2}\right) \tag{4.74}$$

$$P_N = \frac{1}{\lambda} - \frac{\sigma_n^2}{\sigma_N^2} \tag{4.75}$$

4.3 Asymptotic Capacity

One of the key parameters of the communication is its channel capacity, which gives upper limit to data rate. In time-variant channels there are multiple definitions for channel capacity. The maximum mutual information between channel inputs and outputs averaged over

all channel realizations is known as channel capacity. There are many theories, like Shannon's capacity theorem, etc., proposed to calculate channel capacity.

$$C = \log_2 |I + \frac{1}{\sigma_n^2} H R_x H^H| \tag{4.76}$$

$$R_x = E\{x\bar{x}^H\} \tag{4.77}$$

$$R_x = \frac{P_t}{t} I \tag{4.78}$$

$$C = \log_2 |I + \frac{P_t}{t\sigma_n^2} H H^H| \tag{4.79}$$

$$HH^H = \begin{bmatrix} h_1^H & \dots \\ h_2^H & \dots \\ \vdots & \dots \\ h_t^H & \dots \end{bmatrix} \begin{bmatrix} h_1 & h_2 & \dots & h_r \\ \vdots & \vdots & \dots & \dots \end{bmatrix} \tag{4.80}$$

$$= \begin{bmatrix} h_1^H h_1 & h_1^H h_2 & \cdots & \cdots \\ h_2^H h_1 & h_2^H h_2 & \cdots & \cdots \\ \vdots & \vdots & \dots & h_r^H h_r \end{bmatrix}$$

$$h_i^H h_i = \left| |h_i| \right|^2 = t \tag{4.81}$$

$$HH^H = \begin{bmatrix} t & 0 & \dots & 0 \\ 0 & t & \dots & 0 \\ \vdots & \vdots & \ddots & \vdots \\ 0 & 0 & \dots & t \end{bmatrix} = tI \tag{4.82}$$

$$C_a = \log_2 \left(I + \frac{1}{\sigma^2} * \frac{P_t}{t} H H^H \right) \tag{4.83}$$

$$= \log_2 \left(I + \frac{P_t I}{\sigma_n^2} \right)$$

$$= \log_2 \left(1 + \frac{P_t}{\sigma_n^2} \right)^r$$

$$C_a = r \log_2 \left(1 + \frac{P_t}{\sigma_n^2} \right) \tag{4.84}$$

$$= \min(r,t) \log_2 \left(1 + \frac{P_t}{\sigma_n^2} \right)$$

4.4 Introduction to Alamouti Code

To exploit the multiple versions of the data to improve the reliability of data transfer by transferring multiple copies of the data using array of antennas, space-time block coding technique is used. In 1998 Alamouti proposed the simplest space-time block code for the first time but he did not coin the term STBC. It was designed for a 2*2 system. Alamouti code is the only STBC which achieves its full diversity without sacrificing its data rate.

Consider a 2*2 MIMO system:

$$y = [h_1 \quad h_2]\begin{bmatrix} x_1 \\ x_2 \end{bmatrix} + n \tag{4.85}$$

Consider a symbol 'x'.

$$x_1 = \frac{h_1^*}{||h||}x \tag{4.86}$$

$$x_2 = \frac{h_2^*}{||h||}x \tag{4.87}$$

$$\begin{bmatrix} x_1 \\ x_2 \end{bmatrix} = \begin{bmatrix} \frac{h_1^*}{||h||} \\ \frac{h_2^*}{||h||} \end{bmatrix} x \tag{4.88}$$

$$y = [h_1 \quad h_2]\begin{bmatrix} \frac{h_1^*}{||h||} \\ \frac{h_2^*}{||h||} \end{bmatrix} x + n \tag{4.89}$$

$$= ||h||x + n \tag{4.90}$$

$$SNR = \frac{||h||^2 P}{\sigma_n^2} \tag{4.91}$$

$$\begin{bmatrix} \frac{h_1^*}{||h||} \\ \frac{h_2^*}{||h||} \end{bmatrix} x \tag{4.92}$$

First transmit instance

$$y(1) = \begin{bmatrix} h_1 & h_2 \end{bmatrix} \begin{bmatrix} x_1 \\ x_2 \end{bmatrix} + n(1) \tag{4.93}$$

Second transmit instance

$$y(2) = \begin{bmatrix} h_1 & h_2 \end{bmatrix} \begin{bmatrix} -x_2^* \\ x_1^* \end{bmatrix} + n(2) \tag{4.94}$$

$$y^*(2) = \begin{bmatrix} h_1^* & h_2^* \end{bmatrix} \begin{bmatrix} -x_2 \\ x_1 \end{bmatrix} + n^*(2)$$

$$y^*(2) = \begin{bmatrix} -h_1^* & h_2^* \end{bmatrix} \begin{bmatrix} x_2 \\ x_1 \end{bmatrix} + n^*(2)$$

$$y^*(2) = \begin{bmatrix} h_2^* & -h_1^* \end{bmatrix} \begin{bmatrix} x_1 \\ x_2 \end{bmatrix} + n^*(2) \tag{4.95}$$

Stack y(1) and $y^*(2)$ as for receiving info matrix:

$$\begin{bmatrix} y(1) \\ y^*(2) \end{bmatrix} = \begin{bmatrix} \quad \end{bmatrix} \tag{4.96}$$

5. PAPR AND REDUCTION TECHNIQUES

5.1 Peak to Average Power Ratio (PAPR)

5.1.1 Causes of PAPR

OFDM is a multicarrier modulation technique [8]. The major drawback of using OFDM is the presence of high PAPR. The summation operation of the closely spaced subcarriers cause high peak signals compared to the average peaks. The IFFT operation in the transmitter causes PAPR. The complex OFDM symbol is given by equation 5.1.

$$x(k) = \frac{1}{N}\sum_{i=0}^{N-1} X(i) e^{\frac{j2\pi ki}{N}} \tag{5.1}$$

X(i) are the modulated symbols to be given to the IFFT block and x(k) are the k^{th} IFFT sample. The average power of the signal mentioned in equation 5.1 is given by equation 5.2.

$$\text{Average Power} = E\{|x(k)|^2\} = \frac{1}{N^2}\sum_{i=0}^{N-1} E\{|X(i)|^2\} E\left\{\left|e^{\frac{j2\pi ki}{N}}\right|^2\right\} \tag{5.2}$$

$$= \frac{1}{N^2}\sum_{i=0}^{N-1} E\{|X(i)|^2\} = \frac{1}{N^2}\sum_{i=0}^{N-1} a^2$$

$$= \frac{1}{N^2} a^2 N$$

$$= \frac{a^2}{N} \tag{5.3}$$

The average power of transmission is a^2/N. The peak transmission power is a^2. PAPR, which is a fraction of peak power in average power, is given by equation 5.3.

$$\text{PAPR} = \frac{\text{Peak Power}}{\text{Average Power}} = \frac{a^2}{\frac{a^2}{N}}$$

$$= N \tag{5.4}$$

From equation 5.3 it is seen that PAPR depends upon the number of subcarriers. PAPR increases proportionally as the number of subcarriers in IFFT increases. It mainly occurs due to the IFFT preprocessing. Data symbols across subcarriers can add up constructively to produce a signal with a very high peak value. In an OFDM system with 256 subcarriers and modulation of 16 QAM, the PAPR is about 10dB, i.e., 10 times peak power compared to average power. PAPR increases as the number of subcarriers in the IFFT preprocessing increases. PAPR is characterized by the complementary cumulative distribution function (CCDF). It gives a measure about the probability that PAPR value is below a given threshold. CCDF function is described by equation 5.5.

$$F'_X(x) = P(X \geq x) \tag{5.5}$$

$$CCDF = 1 - CDF \tag{5.6}$$

Figure 5.1 shows the PAPR curves for an OFDM system with 256, 128 and 64 subcarriers with a modulation of 16 QAM. From a typical CCDF curve, which follows a chi-square distribution, PAPR can be read as the probability that a certain PAPR value will exceed a threshold for N subcarriers. From Figure 5.1, the probability that PAPR will exceed 10dB for N = 256 is 0.01 or 1% CCDF. From Figure 5.1 it can be seen that as the number of subcarriers increases from 64 to 256, PAPR is also increasing proportionally. This gradual increase can cause adverse effects which are dealt with in the later sections of this chapter.

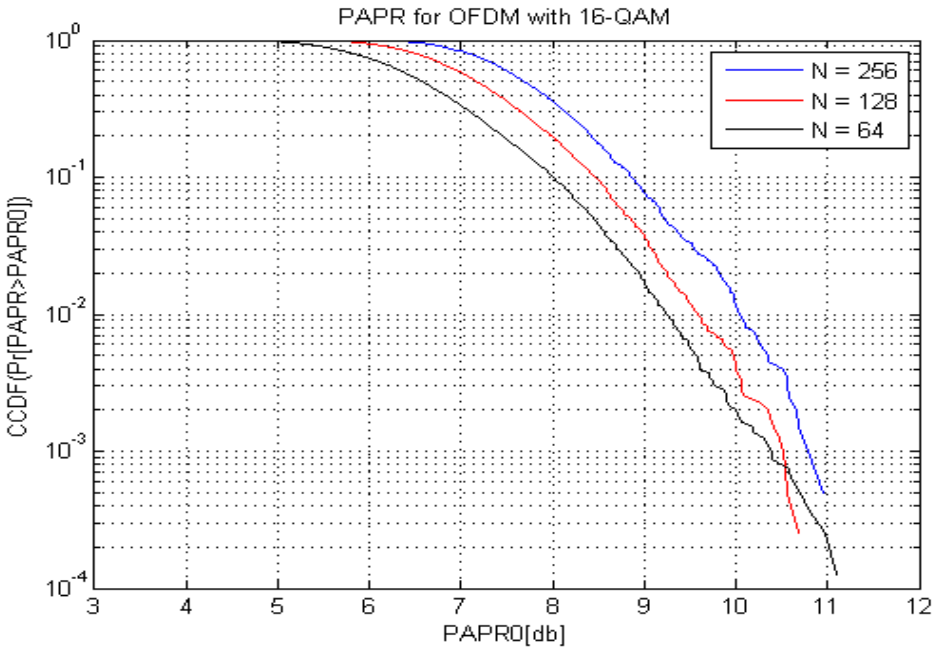

Figure 5.1: PAPR curves for different N values.

However, the type of modulation scheme employed has no effect on PAPR, which can be seen in Figure 5.2.

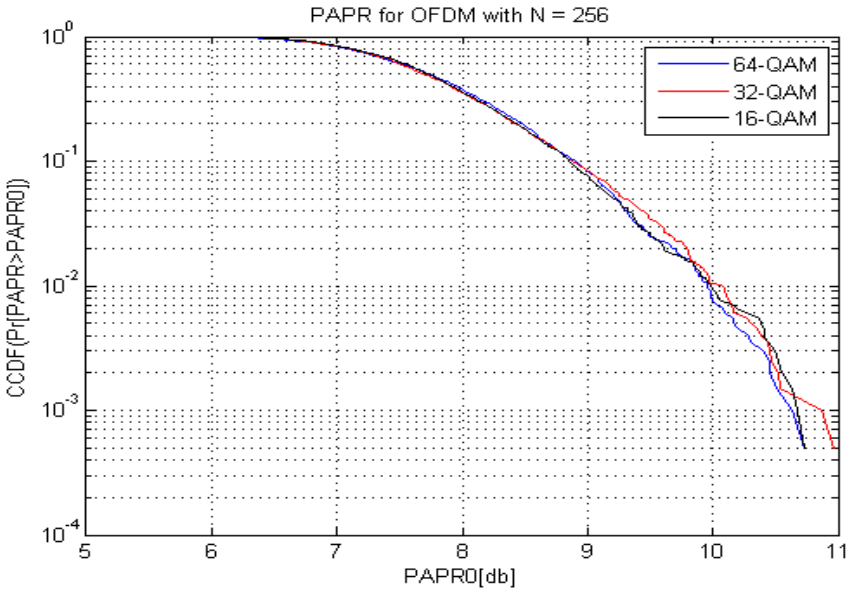

Figure 5.2: PAPR curves for various modulation schemes.

5.1.2 Effect of PAPR

Power amplifiers with certain dynamic range are used in the transmitter before transmitting the signal. Presence of high peaks in the signal will make the peak level go beyond the average level point. The average level point can also be called as the Q-point. When the peak level goes beyond the average level, the amplifier goes into the saturation region. It is no longer functioning in the linear range. The Q-point is now in the saturation range. In this region, the amplifier is totally saturated, leading to signal clipping. The clipped signal has some information loss and the shape of the clipped signal is different from the original one. Amplifier saturation leads to nonlinearity, distortion and inter-carrier interference (ICI). Orthogonality among subcarriers is lost due to clipping, which leads to a very low signal to noise ratio (SNR). Figure 5.3 shows the typical characteristics of an amplifier.

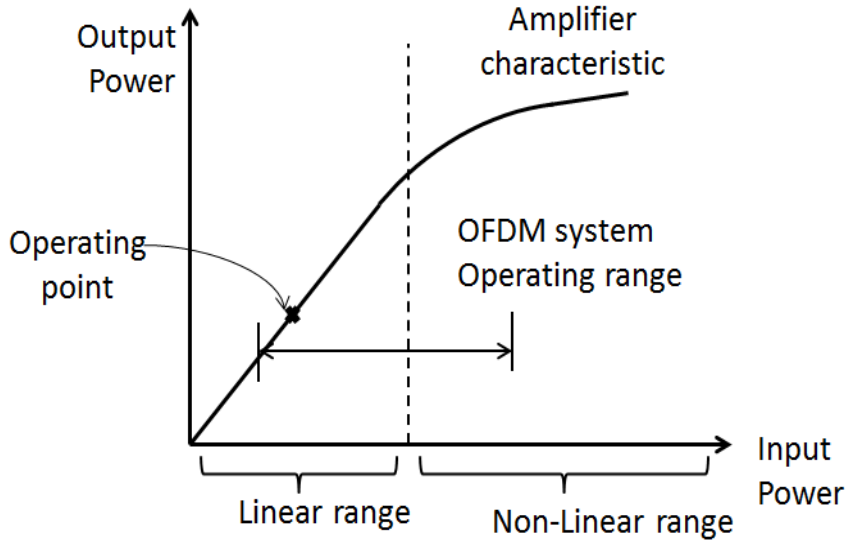

Figure 5.3: Power amplifier characteristics [9].

5.2 Studying PAPR Reduction Techniques

Many techniques have been proposed to reduce the PAPR problem in OFDM. They are classified into different approaches as follows:

1. Signal distortion technique
2. Coding technique
3. Scrambling technique

5.2.1 Signal Distortion Technique

The simplest way to reduce the PAPR is clipping. Clipping and filtering is used at the transmitter to snip the signal at a threshold so as to eliminate the high peaks that are present. Nonlinear saturation is used around the peaks. The peak amplitude now becomes limited to some desired level. By distorting the OFDM signal amplitude, a kind of self-interference is introduced that degrades the BER [10].

The undesired effect of nonlinear distortion can be avoided by doing a linear peak cancellation technique, whereby a time-shifted and scaled reference function is subtracted from the signal such that each subtracted reference function reduced the peak power at least one signal sample. This technique is known as peak window cancellation.

5.2.2 Coding Techniques

Encoding methods employ special forward error correction technique to eliminate high peak signals in OFDM. These schemes include linear block code, Golay code and Reed Muller code [11, 12]. These codes have a few drawbacks as they are not applicable for all OFDM signals. For example, the linear block code is only suitable for small number of subcarriers. Reed

Muller code obtains a low PAPR value but it's limited to only a few types of constellation methods.

As the code rate is reduced coding technique suffers from bandwidth efficiency. Especially for large number of subcarriers, it also suffers from complexity to find the best codes and to store large lookup tables for encoding and decoding.

5.2.3 Scrambling Techniques

The basic idea of symbol scrambling is that for each OFDM symbol, the input sequence is scrambled by a certain number of scrambling sequence, and the output signal with the smallest PAPR is transmitted [13]. This technique also reduces spectral efficiency, and complexity increases as number of subcarriers increases. This is a probabilistic technique and it cannot guarantee PAPR to be below a specified level. Types of symbol scrambling techniques are:

1. Adaptive subcarrier selection: With the subcarrier allocation scheme.
2. Selected mapping (SLM): The transmitter selects one favorable transmit signal from a set of sufficiently different signals which all represent the same information [14, 15].
3. Partial transmit sequence (PTS): The transmitter constructs its transmit signal with low PAR by coordinated addition of appropriately phase-rotated signal parts [8, 9].

CHAPTER 6: STBC MIMO-OFDM AND PAPR REDUCTION

6.1 Introduction

Orthogonal frequency division multiplexing (OFDM) is a multicarrier modulation (MCM) scheme used in 4^{th} generation (4G) communications [8]. This technique is used for high-speed data transmission in mobile communication and digital video broadcasting. OFDM has high spectral efficiency, immunity to inter-symbol interference and capability of handling multipath fading. However, OFDM suffers with a problem called high peak to average power ratio (PAPR). This makes OFDM very sensitive to the nonlinearities in transceiver. A high-power amplifier is designed to work in its saturation region. In this area, nonlinear behavior is severe. The in-band distortions are the sources of these nonlinearities [16]. These in-band distortions will increase the PAPR which in turn reduces the performance of OFDM in the context of bit error rate (BER). So, to preserve the cost-effective advantages of OFDM, reducing the PAPR of OFDM signals is increasingly being considered to be very important.

Using multiple antennas both at transmitter and receiver to enhance the performance is known as MIMO [17]. Due to its ability to withstand high speeds, high capacity and robustness to multipath fading, OFDM combined with MIMO technology with the space-time block coding (STBC) represents an interesting candidate for mobile communication.

Similar to OFDM, the main drawback of MIMO-OFDM with STBC is its high PAPR of the signals transmitted on each antenna. A simple way to reduce this high PAPR is to apply PAPR reduction techniques to each antenna and the side information required to retrace the

signal separately. There are many methods proposed to reduce the PAPR of the OFDM system. Clipping and filtering is the simplest one among them but it increases the bit error rate (BER). Here we are going to look at two signal scrambling techniques for the reduction of PAPR in STBC MIMO-OFDM.

6.2 STBC MIMO-OFDM System

Figure6.1 illustrates the general block diagram of STBC MIMO-OFDM system. Baseband modulated symbols are passed through serial to parallel converter which generates a complex vector of size N. Then this vector is passed through STBC encoder. The output sequences of STBC encoder are then passed through each IFFT block for antenna as 1 and 2 respectively.

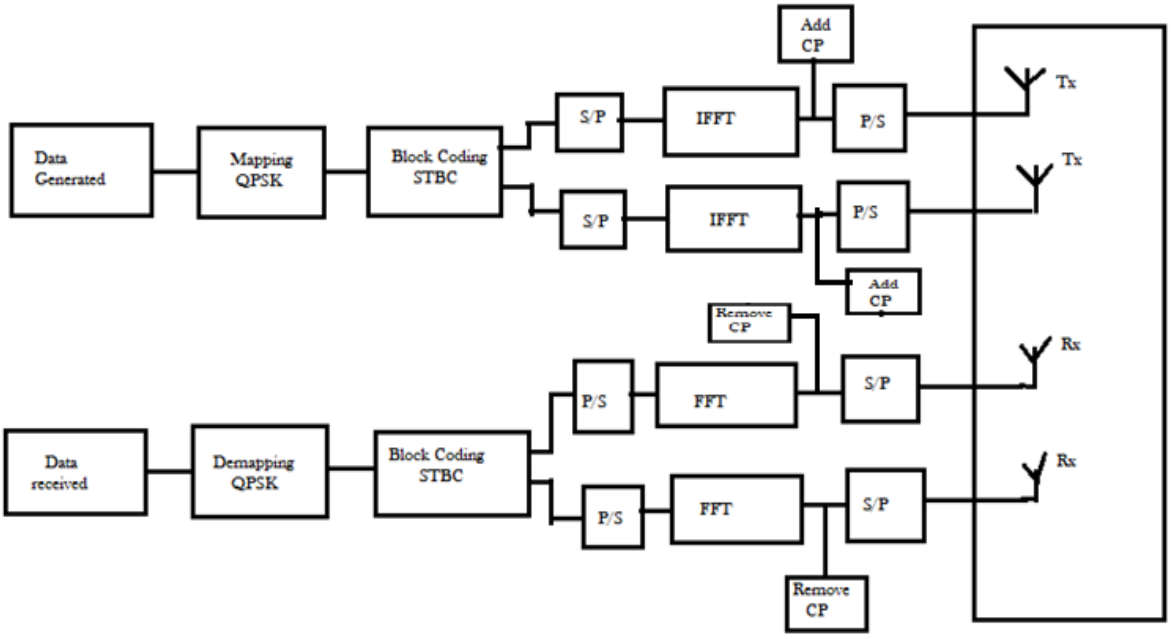

Fig. 6.1 Structure of STBC MIMO OFDM.

6.3 Alamouti Space-Time Block Coding (STBC)

Nowadays in wireless communications, increasing transmission rates and providing robustness to channel conditions are the two of the main research topics. So, the main aim of the research is to develop systems that offer both high speed and capacity. Much effort is done in the area of multiple input multiple output (MIMO) systems. By using space-time codes such as Alamouti code in a multi-antenna system, we can exploit space and time diversity.

Space-time coding technique is essentially a two-dimensional (2-D) space and time processing method [14]. The receiver antennas can realize diversity reception because of the introduction of correlation of time and space between signals which are transmitted by different antennas. So, space-time coding is especially used for enhancing the capacity of a wireless system without using more bandwidth [10, 18].

In this thesis, we used Alamouti space-time block coding to achieve spatial diversity in MIMO system. In this technique, every two continuous transmit symbols s_1 and s_2 are coded into a transmit symbol matrix as follows:

$$s = \begin{bmatrix} s_1 & -s_2^* \\ s_2 & s_1^* \end{bmatrix} \tag{6.1}$$

where s is the space-time code with its columns representing space dimensions while rows represents time dimension [11]. Alamouti encoded signal is then transmitted through two transmit antennas simultaneously. During the first symbol period, s_1 and s_2 are transmitted simultaneously, and during the second symbol duration, $-s_2^*$ is transmitted from first antenna and s_1^* is transmitted from second antenna.

6.4 PAPR Reduction Techniques

6.4.1 Selected Mapping Method (SLM)

In selected mapping, U statistically independent sequences are generated which represent the same space-time coded OFDM symbol [9, 14]. The probability of PAPR greater than a certain threshold is given by

$$\text{Prob}(\text{PAPR} > \text{Z}) = 1 - (1 - \exp(-\text{Z}))^{\text{N}}$$

The probability of PAPR>Z for 'U' statistically independent sequences is given by

$$(\text{Prob}(\text{PAPR} > \text{Z}))^{\text{U}} = (1 - (1 - \exp(-\text{Z}))^{\text{N}})^{\text{U}} \quad (6.2)$$

The message symbols S(n) are duplicated U number of times and each copy is passed into phase rotation block as shown in Figure 6.2. The U statistically independent data blocks $S_1(n)$, $S_2(n)$,….$S_U(n)$ are thus generated by multiplying S(n) with U phase rotation vectors $P_1(n)$, $P_2(n)$,….$P_U(n)$.

$$P_u(n) = e^{j\Phi_n^{(U)}}, \ \Phi_n^{(U)} \in [0,2\pi], \ n = 1:N, \ u = 1:U \quad (6.3)$$

$$S_u(n) = S(n)e^{j\Phi_n^{(u)}} \quad (6.4)$$

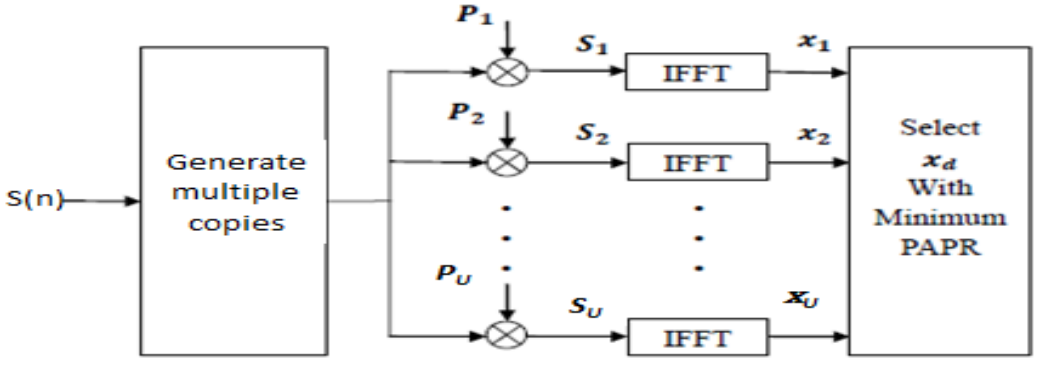

Figure 6.2: Block diagram of SLM technique [9].

The multiple copies of sequence S(n) are fed to IFFT block where modulation takes place and then the output x_1, x_2,…….x_U is generated. The PAPR of each modulated sequence is calculated independently and finally the sequence x_d where ($1 \leq d \leq U$), which is the lowest PAPR, is selected for transmission through the channel.

$$x_d = \text{argmin}_{(1 \leq d \leq U))} \text{PAPR}(x_U) \quad (6.5)$$

Since the multiple copies containing the same information are statistically independent, the PAPR performance of MIMO-OFDM system is improved significantly. Assuming the probability of PAPR > threshold for a single signal is p; then for U copies generated, the CCDF probability becomes p^U. Thus statistically the PAPR performance of OFDM is improved using SLM technique. In order to correctly demodulate the received signal, we need to send the side information which contains information about which phase vector sequence was selected needs to be transmitted to the receiver. This can be done by sending $N_{SLM} = \log_2 U$ bits, which are used to represent the route number U.

SLM Scheme Simulation Steps

1. Symbols were generated using M-QAM modulation where M is the size of constellation. Space-time coded symbols are generated by passing symbols through Alamouti encoder.
2. N-point IFFT was taken for modulation where N = 128 i.e., number of subcarriers in OFDM system. A total of 2500 space-time coded OFDM symbols were generated and PAPR was calculated for each symbol to plot CCDF curve of original OFDM symbols.
3. Phase factor set P was generated, and to reduce complexity, only four values were chosen for the P vector [1,-1, j,-j].

4. Multiple copies 'U' were generated for each space-time coded OFDM symbol and each copy was multiplied with a phase vector or rotation factor. From U copies the lowest PAPR copy was selected for transmission for each symbol.
5. Simulations were done for different values of U (2, 4, 8, and 16) and from the results it is a fact that the PAPR reduction performance improved as the value of U increased.

6.4.2 Partial Transmit Sequence (PTS)

Muller and Huber [14] first proposed the PTS method for improving the statistics of the OFDM signal. It is a non-distortion technique. In PTS technique the original space-time coded OFDM signal is divided into V-equal number of non-over lapping sub-blocks. Then each sub-block is multiplied with different phase rotation factors and then added. This process is repeated until optimum values of phase factor combination are found which result in lowest PAPR. The block diagram of PTS technique is shown in Figure 6.3.

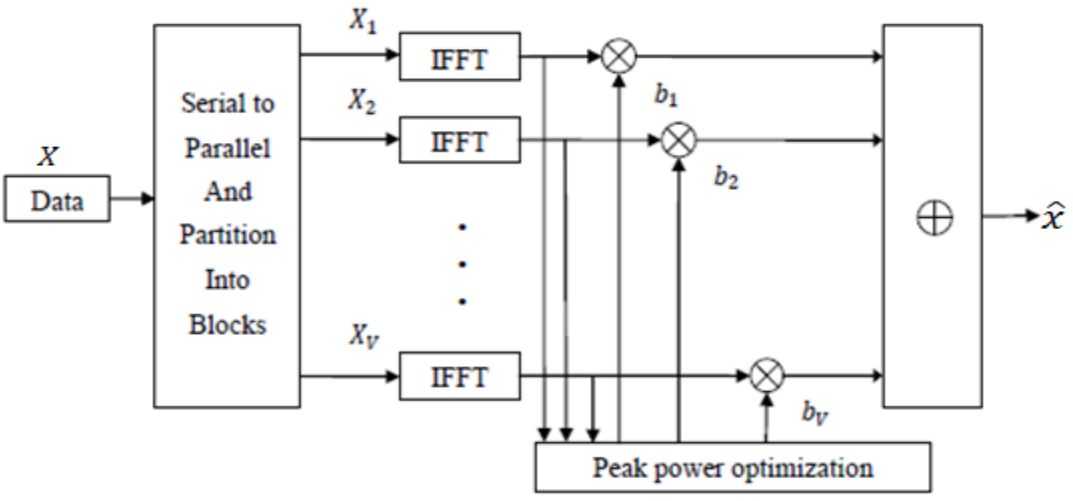

Figure 6.3 Block diagram of PTS technique [14].

The data or information signal X is given as input to serial to parallel converter (S/P) and partitioning block where signal is converted to parallel and partitioned into V non-overlapping sub-blocks [X_1,X_2,…..X_V]. These are then passed to the IFFT block where they are converted into time domain (modulation). Phase factor b_v is multiplied with respective sub-block as shown in equations below:

$$X = \sum_{v=1}^{V} X_v \tag{6.6}$$

$$\hat{x} = \sum_{v=1}^{V} b_v x_v \tag{6.7}$$

$$b_v = e^{j\Phi_v}, \Phi_v \in [0,2\pi] \tag{6.8}$$

Where b_v is the phase rotation factor.

The above procedure is repeated by selecting different values for phase factor combination [b_1, b_2,…b_v] and the optimum combination which gives the lowest PAPR is selected for transmission. Thus by finding the optimum phase factor combination [b_1, b_2,…b_v] we can reduce PAPR of each OFDM symbol as shown in equation 6.9.

$$\hat{b} = \{\hat{b}_1, \hat{b}_2 \dots\dots \hat{b}_V\} = \underset{(b_1,b_2\dots b_v)}{\operatorname{argmin}} \max_{1\le n\le N} \left|\sum_{v=1}^{V} b_v x_v\right|^2 \tag{6.9}$$

In this algorithm we perform V-1 times extra IFFT operation. B = [b_1, b_2,… b_v] is set of V discrete values. Suppose Φ_v has W different values then b will have $V.W^V$ different combinations. So as V increases W increases, hence computational cost increases and PAPR is further reduced. Side information that needs to be transmitted is (V-1).log2W. If b_v contains only four possible values [±1, ±j] (W=4) then computational complexity is reduced as side info = (V-1)*2. This is usually done in practice in order to reduce the computation burden.

PTS Scheme Simulation Steps

1. Symbols were generated using M-QAM modulation where M is the size of constellation. Space-time coded symbols are generated using Alamouti encoder.
2. To perform modulation, N-point IFFT is done where N – is number of subcarriers, i.e., 128 in this case. A total of 2500 OFDM symbols were generated and PAPR was calculated for each OFDM symbol to plot CCDF curve of original OFDM symbols.
3. Different values of V (number of sub-blocks) and W (number of values b can take) are considered for simulation.
4. By keeping W constant, simulations were done for different values of V (2, 4, and 8). Space-time coded OFDM symbol was portioned into V number of sub-blocks and IFFT was applied for each sub-block. Then phase factors = $[b_1, b_2, \ldots b_v]$ were multiplied with each sub-block and added. PAPR was calculated for each combination and lowest PAPR was chosen. This was repeated for all space-time coded OFDM symbols.

CHAPTER 7: SIMULATION RESULTS AND ANALYSIS

PAPR reduction techniques discussed in Chapter 6 are simulated and analyzed using MATLAB 2012R2b.

7.1 SLM Scheme Simulation

Scrambling techniques were simulated first. The selective mapping technique generates multiple copies of the STBC OFDM symbol. The simulation parameters are given in Table 7.1. The selected mapping technique SLM scheme shows a much better PAPR reduction than the original STBC OFDM symbol. The PAPR reduction performance improves as the number of SLM copies generated increases as shown in Figure 7.1.

As more copies of space-time coded OFDM symbol are generated (i.e., the value of M is increased), PAPR is reduced further. The reduction in PAPR becomes less significant beyond M>8. This shows there won't be a linear growth if PAPR reduction performance. The bit error rate performance is not affected much with SLM technique implementation. There was a slight decrease in bit error rate where E_b/N_o>10dB compared with original bit error rate plot.

SLM requires 'M' IFFT operations at transmitter; hence computational complexity increases. M number of IFFT operations for N points require $n_{mul} = M * \frac{N}{2} * \log_2 N$ complex multiplications and $n_{add} = M * \frac{N}{2} * \log_2 N$ complex additions. Hence for practical applications a compromise between PAPR reduction and computational complexity is achieved by choosing value of M≤8. Log_2M bits need to be sent to the receiver in the form of side information in order to correctly decode the low PAPR OFDM symbol are required to explicitly represent side info.

Figure7.2 shows the BER performance of space-time coded MIMO-OFDM with SLM scheme with U = 4.

Table 7.1 Simulation Parameters for SLM Scheme

Modulation format	4-QAM
Number of subcarriers	128
Number of symbols generated	2500
Phase vector	[1,-1,j,-j]
OFDM symbol copies 'U'	[2,4,8,16]

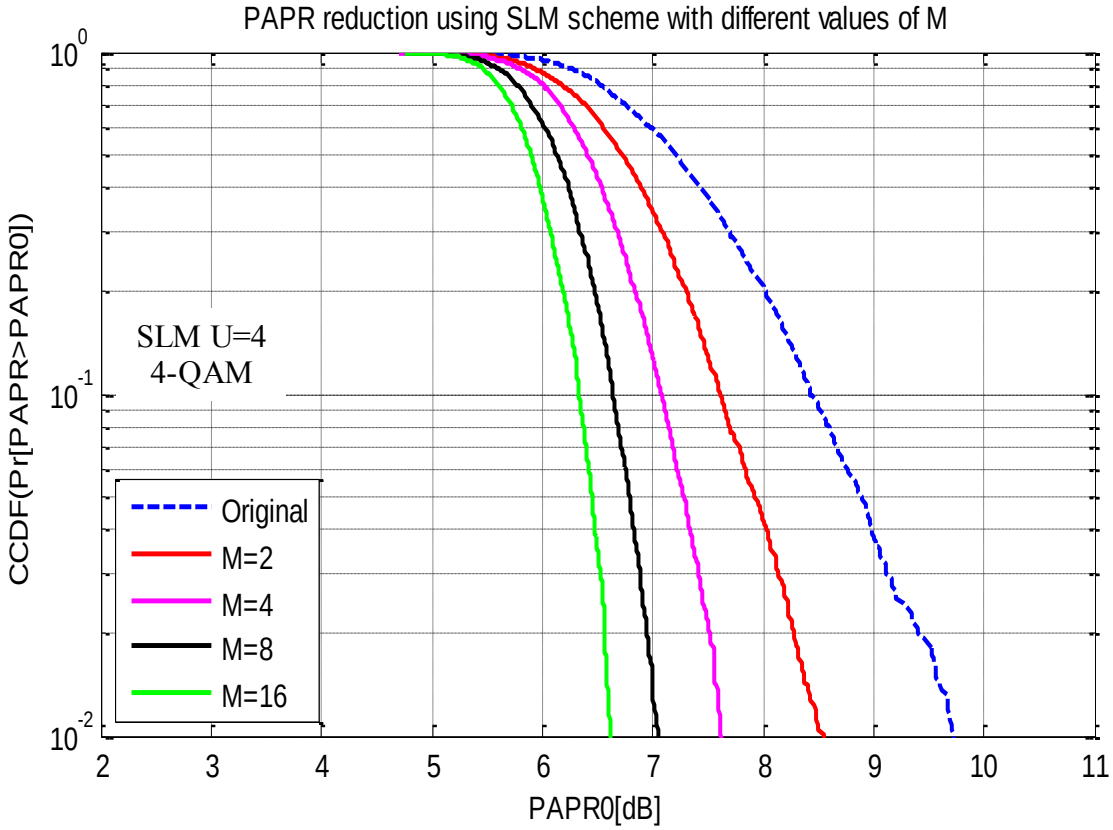

Figure 7.1 PAPR reduction performances with different values of M.

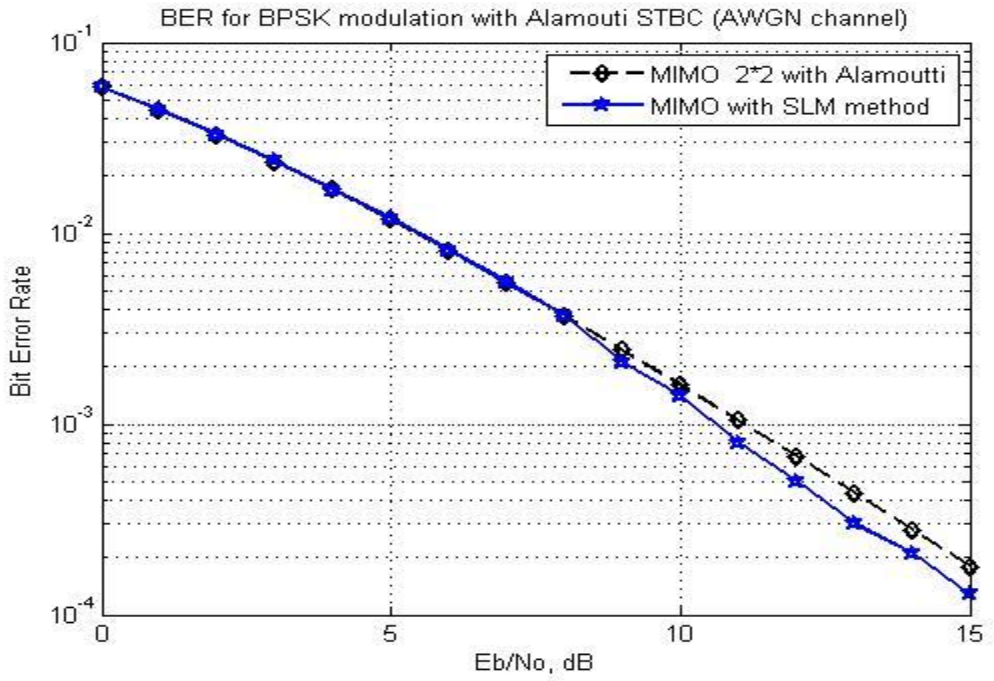

Figure 7.2 BER graph for SLM method with U = 4.

7.2 PTS Scheme Simulation

Simulations are done for multiple values of V, i.e., number of sub-blocks. The simulation parameters used are shown in Table 7.2. A much better PAPR reduction is obtained using PTS scheme when compared with the original OFDM symbol. PTS gives better and better performance as the number of sub-block partitions increase as shown in Figure 7.3. As the value of V is increased beyond 8, the PAPR reduction becomes less significant. This shows there is a nonlinear growth in PAPR reduction as number of sub-blocks is increased.

PTS requires 'V' IFFT operations at transmitter; hence computational complexity increases. V IFFT operations for N points require $n_{mul} = V * \frac{N}{2} * \log_2 N$complex multiplications and $n_{add} = V * \frac{N}{2} * \log_2 N$ complex additions. Figure 7.4 shows BER performance is increased with PTS scheme.

Table 7.2 Simulation Parameters for PTS Scheme

Modulation format	4-QAM
Tx IFFT size (N), number of subcarriers	128
Number of OFDM symbols generated	2500
Phase vector b	W=4 [1,-1,j,-j]
Number of sub-block partitions 'V'	[2,4,8]

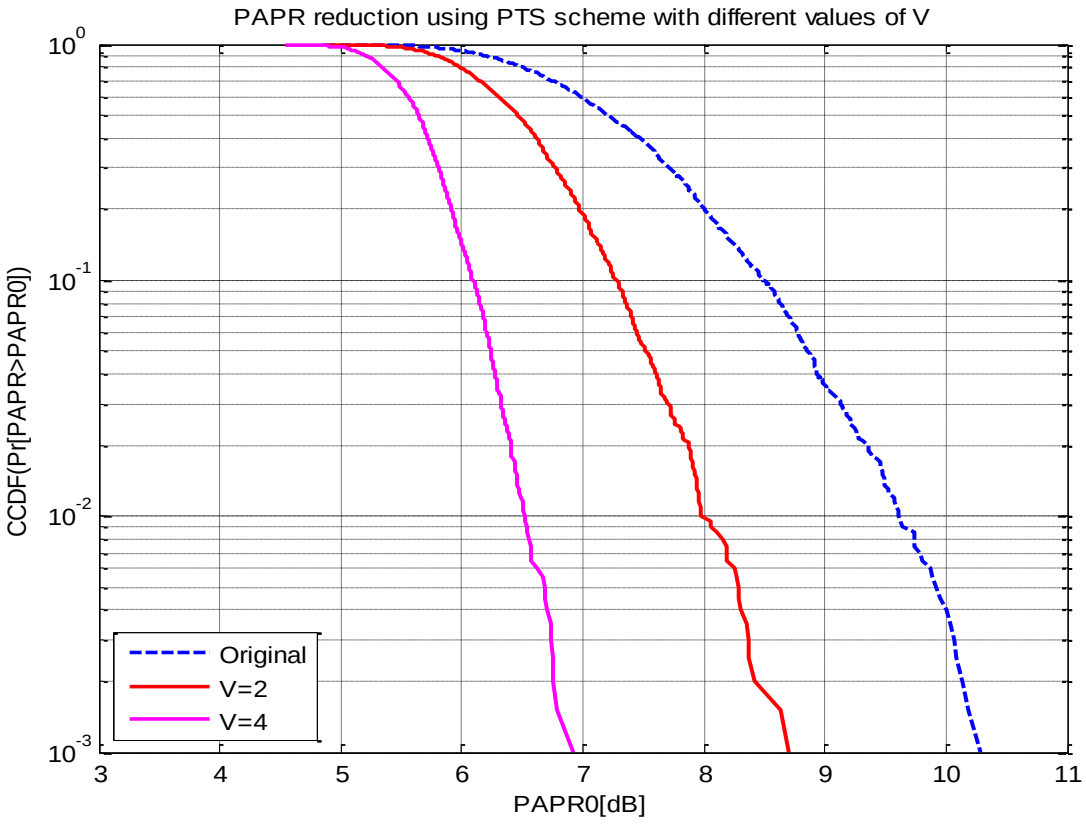

Figure 7.3 PAPR reduction performances of PTS with different values of V.

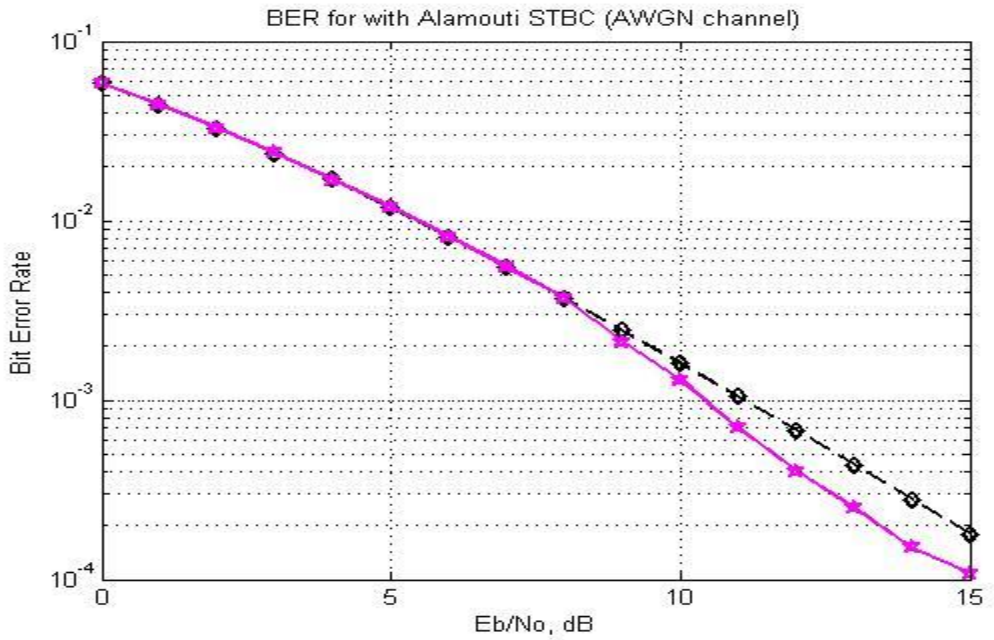

Figure 7.4 BER performance of PTS for V = 4.

7.3 Comparative Analysis

Scrambling techniques were compared as shown in Figure 7.5. The number of copies in SLM and number of sub block divisions were kept the same for a fair comparison. PTS technique gives a better performance than SLM technique and the number of information bits required to be sent in PTS technique is more. Table 7.3 shows the comparison of the two scrambling techniques. Figure7.6 shows the bit error rate comparison graph of MIMO-OFDM with SLM and PTS scheme. From the Figure7.6, it is evident that, PTS scheme gives better performance than SLM scheme.

Table 7.3 Comparison of PAPR Reduction Performance of SLM and PTS Schemes

V = U =4	No. of IFFT required	Info bits required	Phase vector set	PAPR(dB) at 1% prob.
SLM	4	2	[±1, ±j]	7.6
PTS	4	2	[±1, ±j]	6.9

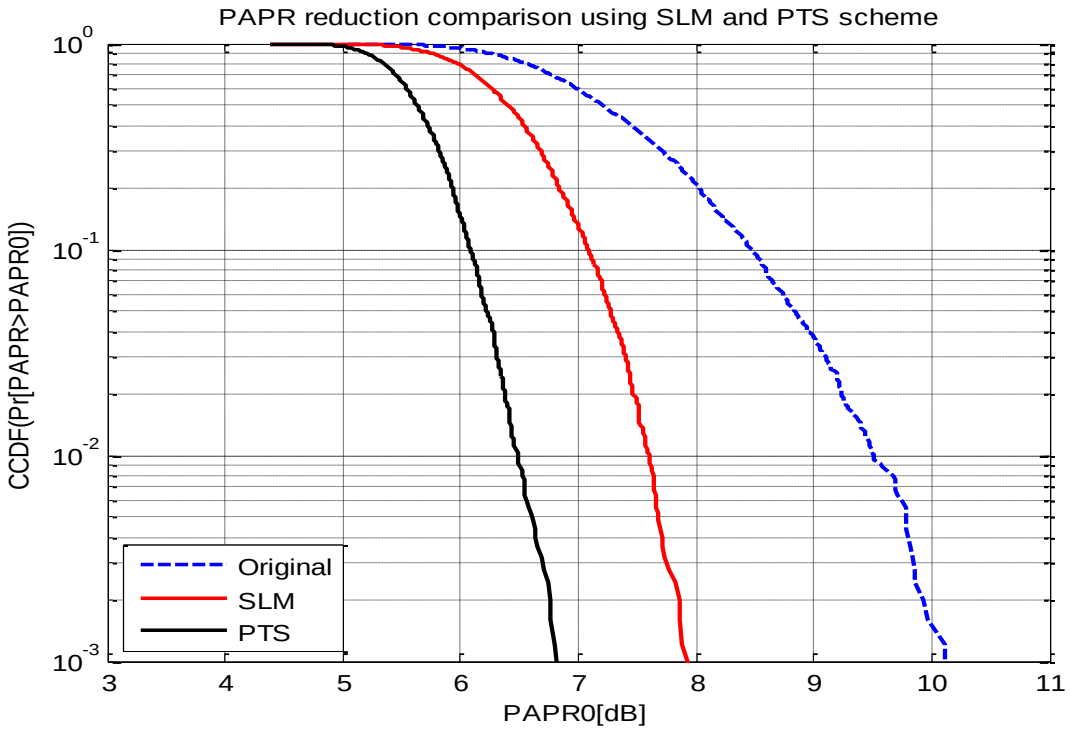

Figure 7.5 Comparison of PAPR reduction performance using SLM and PTS schemes.

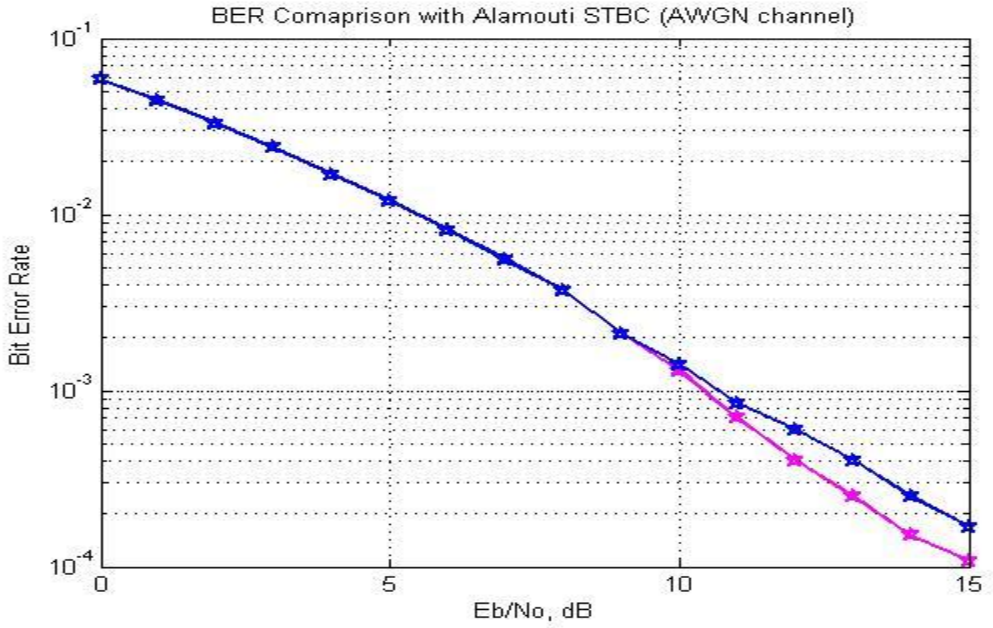

Figure 7.6 Comparision BER of STBC MIMO-OFDM with SLM and PTS.

The bit error rate performance of different MIMO-OFDM systems are compared with each other. Figure.7.7 clearly shows that SIMO (single transmitter antenna and two receiving antennas) performs better than MIMO (two transmit and receiving antennas) and MISO (two transmit and one receiving antenna). MIMO is performs better than MISO.

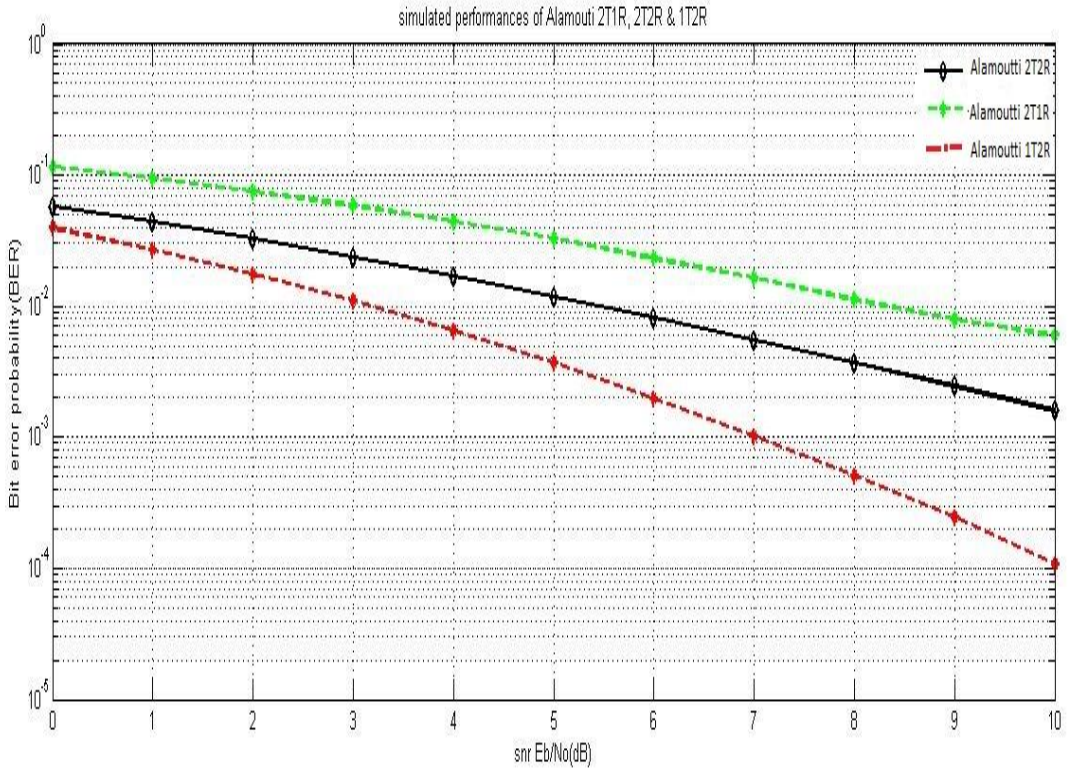

Figure 7.7 BER comparision for SIMO, MISO and MIMO.

CHAPTER 8: CONCLUSION AND FUTURE WORK

8.1 Conclusion

PAPR increases as the number of subcarriers is increased. STBC OFDM symbol was generated using different modulation schemes like BPSK, QPSK, 4-QAM, 16-QAM, and 64-QAM and then by using Alamouti coding. There was insignificant change in PAPR with different modulation schemes.

PAPR reduction techniques for MIMO-OFDM system with space-time block coding were simulated and compared with each other. PTS gives the better performance when compared with SLM.

The bit error rate (BER) vs. signal to noise ratio (SNR) performance of SLM and PTS schemes was simulated and compared. SLM and PTS techniques performance was the same. As the size of constellation for input modulation increased from M=4 to 64 there was a significant degradation of BER performance.

8.2 Future Work

The future work may include channel estimation and synchronization blocks in MIMO-OFDM system. Advantages of combining PAPR reduction techniques with orthogonal space-time block-coding (OSTBC) can be explored. The receiver part of MIMO-OFDM system may be simulated and analyzed using different receivers for future work since this thesis deals with only the transmission of MIMO-OFDM symbol and zero forcing receiver. Future work may include spatial multiplexing using space-time coded MIMO-OFDM.

REFERENCES

[1] Dwivedi, S.K., Paulus, R., Jaiswal, A.K., and Kumar A, April 2014, "Evaluate the PAPR and BER Performance of SCFDMA with NCT Technique," *International Journal of Current Engineering and Technology*, India, E-ISSN 2277-4106, P-ISSN 2347-5161, Vol. 4, No. 2, pp. 1000-1003.

[2] Verma, P., and Sharma, N., September 2012, "IFDMA-Promising Technique for 3G/4G," *International Journal of Electronics and Computer Science Engineering*, P. Verma et al., eds.,India, ISSN 2277-1956, Vol. 1, No. 4, pp. 2207-2216.

[3] Salah, M., Abdel-Fadeel, G., and Nossair, Z.B., May 26-28, 2009, "Peak to Average Power Ratio Reduction in Single Carrier OFDMA Systems," *13th International Conference on Aerospace Sciences and Aviation technology (ASAT-13)*, ASAT-13-CM-14, Cairo, Egypt.

[4] Jagannatham, A.K., "Wireless Channel and Fading." Lecture 2 in Advanced 3G and 4G Wireless Mobile Communications (online course). Indian Institute of Technology, Kanpur, India. Retrieved 01/10/2014. http://nptel.ac.in/courses/117104099

[5] Jagannatham, A.K., "Wireless Channel and Delay Spread." Lecture 9 in Advanced 3G and 4G Wireless Mobile Communications (online course). Indian Institute of Technology, Kanpur, India. Retrieved 01/10/2014. http://nptel.ac.in/courses/117104099

[6] Jagannatham, A.K., "Introduction to OFDM and Multicarrier Modulation." Lecture 27 in Advanced 3G and 4G Wireless Mobile Communications (online course). Indian Institute of Technology,Kanpur, India. Retrieved 01/10/2014. http://nptel.ac.in/courses/117104099

[7] Weinstein, S., Ebert, P., October 1971, "Data Transmission by Frequency Division Multiplexing Using the Discrete Fourier Transform," *Communication Technology, IEEE Tran.*, Vol.19, No.5, pp. 628-634.

[8] R.Prasad, OFDM for Wireless Communications Systems[M]. Boston, MA. Artech. House Publishers, 2004.

[9] R.W.Bami, R. F. H. Fischer, and J. B. Huber, "Reducing the peak to average power ratio of multicarrier modulation by selective mapping," *Electron. Lett*., vol. 32, no. 22, pp. 2056–2057, Oct. 1996.

[10] A. E. Jones, T. A.Wilkinson, and S. K. Barton, "Block coding scheme for reduction of peak-to-average envelope power ratio of multicarrier transmission systems," Electron. Lett., vol. 30, no. 25, pp. 2098–2099, Dec. 1994.

[11] J. A. Davis, J. Jedwab, "Peak-to-Mean power control and error correction for OFDM transmission using Golay sequences and Reed-Muller codes," *IEEE Electronic Letters*, vol. 33, no. 4, Feb 1997, pp. 267-268.

[12] Leonard J. Cimini, Jr., Nelson R. Sollenberger, "Peak-to-Average power ratio reduction of an OFDM signal using partial transmit sequences," *IEEE Electronic Letters*, vol. 4, no. 3, Mar 2000, pp. 88-86.

[13] Myung, H.G., and Goodman, D.J., 2008, "Single Carrier FDMA: A New Air Interface for Long Term Evolution," John Wiley & Sons, Ltd., New York, 2008. doi: 10.1002/9780470758717

[14] S. H. Muller and H. B. Huber, "OFDM with reduced peak-to-mean power ratio by optimum combination of partial transmit sequences," *Electronics Letters*, vol. 33, pp. 368-369, Feb. 1997.

[15] W. Yi, G. Linfeng "An Investigation of Peak-to-Average Power Reduction in MIMO-OFDM Systems," Oct. 2009.

[16] Jagannatham, A.K., "ISI in Wireless Communications." Lecture 11 in Advanced 3G and 4G Wireless Mobile Communications (online course). Indian Institute of Technology, Kanpur, India. Retrieved 01/10/2014. http://nptel.ac.in/courses/117104099

[17] Jagannatham, A.K., "MIMO OFDM and Multicarrier Modulation." Lecture 31 in Advanced 3G and 4G Wireless Mobile Communications (online course). Indian Institute of Technology, Kanpur, India. Retrieved 01/10/2014.http://nptel.ac.in/courses/117104099

[18] Radhia Gharsallah, Ridha Bouallegue "Combined with space-time coding multi-user detection for CDMA-OFDM/OQAM SYSTEM" International Journal of Wireless and Mobile Networks (IJWMN) Vol.4, No.4, August 2012.